一週一話
One topic a week

ロボットスーツHALによる歩行改善効果の可能性

国立病院機構新潟病院副院長
中島　孝

随意運動障害の改善

随意運動障害をきたす病気には脳血管障害，脊髄損傷や神経・筋難病があり，根治療法の開発のみならず，ambulation disorder（歩行不安定症）の治療方法を研究する必要がある。

随意運動は人が内的環境を自ら整え，主体的に生きる際の重要な機能であり，その治療法として，脳卒中モデルをもとにした反射階層理論（Brunnstrom, 1970），ポリオモデルをもとにした固有受容性神経筋促通法（PNF），脳性麻痺モデルから導かれたBobath法などが古くからあるがエビデンスは十分ではない。新しい理論と方法に促通反復療法（Kawahira, 1997），機器を使った方法にTES/FES（治療的/機能的電気刺激）や，本稿で扱う筑波大学の山海嘉之教授の提唱するcybernics（サイバニクス）がある。サイバニクスでは運動プログラム理論（Bernstein, 1967）で想定された理想的な神経・筋系の再プログラミングを現実に行うことができる可能性がある。

サイバニクスとは何か？

サイバニクスはcybernetics, mechatronics, informaticsを融合し，装置と人の身体/脳がリアルタイムに情報交換して人を支援する技術概念であり，それに基づく装置が，生体電位駆動型装着型ロボット，すなわち皮膚表面に表れる生体電位信号（bioelectric signal）から装着者の随意運動意図を解析し，各種センサー情報と運動パターンのデータベースを参照し，適切なモータトルクで随意運動を増強するHAL（hybrid assistive limb）である。補装具としてのHALは健康な人の身体機能を増強する特徴があり，普通は持ち上げられない重い物を持ち上げることができる。

山海はiBF仮説（interactive bio-feedback hypothesis）すなわち，"動作意思を反映した生体電位信号によって動作補助を行うロボットスーツHALを用いると，HALの介在により，HALと人の中枢系と末梢系の間で人体内外を経由してインタラクティブなバイオフィードバックが促され，脳・神経・筋系の疾患患者の中枢系と末梢系の機能改善が促進されるという仮説"を提唱しており，そこからHALによる随意運動回復訓練が考えられた。脳・脊髄・運動神経・筋の障害から来る歩行不安定症に対して，患者がHALを装着して定期的に歩行練習を行うことで，HALを脱いだ後の歩行改善効果（neuromuscular plasticity）が期待されている。

HALの動作メカニズムと実装

HALは，装着者の随意運動意図に基づき動作するサイバニック随意制御（CVC），HAL内部の運動データベース（例：起立，歩行，走行など）を参照し生体電位信号が不十分でも運動を完成させるサイバニック自律制御（CAC），装着者に重さを感じさせないサイバニックインピーダンス制御（CIC）により構成されている[1]。

HAL®下肢用（NON-MEDICAL）とHAL®下肢用（MEDICAL）はサイバーダイン株式会社で開発・製造されており，前者は日本国内の医療または福祉施設で利用することができる。後者は，神経・筋疾患などで特徴的な生体電位信号（運動単位として微弱でまばらな電位）の検出・処理機能が実装され，最も難度の高いと思われる疾患に適合させることで，脳卒中や脊髄損傷を含む脳・脊髄・神経・筋疾患によるあらゆる歩行不安定症に対応している。医療機器品質保証のための国際標準規格ISO 13485に基づいて製造され，EUの医療機器としてのCE0197を取得している（2013年8月）[1)2)]。

HALの臨床応用と今後

脳卒中片麻痺患者に対して，HAL下肢用（NON-MEDICAL）の臨床研究が行われ，10m歩行テストでスピード，ケイデンスの有意な改善効果が認められた[3]。ドイツでは不全脊髄損傷に対する，HAL下肢用（MEDICAL欧州モデル，HAL-ML05）を使った歩行練習によって歩行改善効果が得られ，労災保険適用が認められた[2]。

日本でも同様のモデルを使用して，厚生労働省難治性疾患等克服研究事業において，薬事法に基づく多施設共同医療機器治験「希少性神経・筋難病疾患の進行抑制治療効果を得るための新たな医療機器，生体電位等で随意コントロールされた下肢装着型補助ロボット（HAL-HN01）に関する医師主導治験―短期効果としての歩行改善効果に対する無作為化比較対照クロスオーバー試験：NCY-3001試験」が2013年3月から行われている。

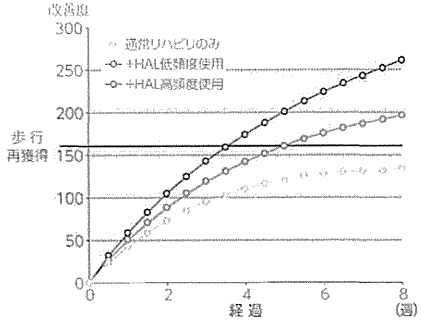

図1　HALを使った回復曲線の想定（脳血管障害，脊髄損傷モデル）
図は通常リハビリでは歩行を再獲得できないが，HALを使えば使うほど，より早期に歩行が再獲得できる可能性を示すシミュレーション例

この目的は緩徐進行性の希少性神経・筋難病患者の歩行不安定症が短期間，間欠的にHAL-HN01を治療的装着することで改善するという有効性・安全性を検証することである。対象疾患例としては，脊髄性筋萎縮症，球脊髄性筋萎縮症，下肢症状が緩徐進行性のALS，シャルコー・マリー・トゥース病，遠位型ミオパチー，封入体筋炎，先天性ミオパチー，筋ジストロフィーおよび診断が確定していないが，上記病態と同等とみなされるものである[2]。

脳血管障害や脊髄損傷など急性疾患では図1のように，通常リハビリでは歩行再獲得が不可能であっても，HALを使えば使うほど，歩行が早期に再獲得できる可能性がある。進行性の病態に対して，薬剤とHALを複合療法（combined therapy）として使うことで，さらなる改善を得られる可能性がある[2]。

●文　献
1）中島　孝：保健医療科．2013；60(2)：130-7．
2）中島　孝，他：治療．2013；95(12)：2088-93．
3）Kawamoto H, et al:BMC Neurol. 2013;13:141.

2015年2月2日
第3111号

週刊（毎週月曜日発行）
購読料1部100円（税込）1年5000円（送料、税込）
発行＝株式会社医学書院
〒113-8719 東京都文京区本郷1-28-23
TEL(03)3817-5694 FAX(03)3815-7850
E-mail：shinbun@igaku-shoin.co.jp
JCOPY 《社出版者著作権管理機構 委託出版物》

New Medical World Weekly
週刊 医学界新聞
医学書院 www.igaku-shoin.co.jp

今週号の主な内容

対談 ロボットスーツHAL®は医療をどう変えるのか

川口 有美子氏＝聞き手
NPO法人ALS/MNDサポートセンター さくら会 副理事長

中島 孝氏
国立病院機構新潟病院 副院長・神経内科

世界をリードする日本のロボット技術。その粋を集めたロボットスーツHAL®（Hybrid Assistive Limb®，以下HAL）を，医療機器として利用する未来が見えてきた。

本紙では，神経・筋疾患患者を対象に「HAL-HN01（医療用HAL）」を利用した治療の医学的効果の検証を試みる中島孝氏と，難病である筋萎縮性側索硬化症（ALS）をテーマとした著書『逝かない身体』を持つ川口有美子氏との対談を企画。HALとは何か，HALを用いた治療ではどのような医学的効果が期待できるのか。中島氏が研究代表者を務めた治験の内容を足掛かりに，HALを用いた治療によって患者にどのような福音がもたらされるかに迫った。

川口 先日，国立病院機構新潟病院へ伺い，難病患者さんたちがHALを着用して歩いている様子をようやく見ることができました。印象的だったのが，患者さんたちの楽しそうな雰囲気です。「HALは患者さんのQOLを高めるものになるに違いない！」って直感しました。

中島 ご覧になったのはHAL下肢用のHAL-FL05でしたね。おっしゃるとおり，HALを装着して歩行プログラムに成功した患者さんは皆，笑顔になるんです。治験（MEMO）においては医療機器としての治療効果とともに，その笑顔になる患者さんの主観の部分にもフォーカスした評価研究を進めてきました。

川口 今日はそのあたりもぜひ伺いたいと思っています。

「操作する／される」とは異なる，身体と機器の協働を実現

川口 まず，HALが一体どういうものであるのか。そこから共有させてください。

中島 HALは四肢に装着する外骨格型の装着型ロボットで，人間の身体機能を改善・補助・拡張することのできる世界初のサイボーグ型ロボットです。筑波大大学院教授であり，サイバーダイン社CEOの山海嘉之氏が1991年から研究に着手し，発明に至りました。

川口 Cybernetics（サイバネティクス），Mechatronics（メカトロニクス），Infomatics（インフォマティクス）を融合した「Cybernics（サイバニクス）」という概念を基に作り上げたものであるとお聞きしました。

中島 Cybernicsはまさに HALの基本的な原理に当たると思います。人が機械を操作するサイバネティクスと異なり，HALには機器を操作する操縦桿やボタン，キーボードはありません。機器を装着し，電線で直接結ばれることによって，人と機器との情報交換をリアルタイムに行えるようになる。すると，その人の意思通りに，機器と身体を動かすことができるようになるのです。

「人が機器を操作する」「機器が人を動かす」とも違い，「人と機器が協働する」というニュアンスで理解していただくことがふさわしいと言える技術です。

一体感を生む，HALの3機能

川口 機器を使うわけでもなく，機器に使われるわけでもない――。まさに人と機器の融合が可能になっている，と。具体的にはどのような機能により，それが実現できているのですか。

中島 ①「サイバニック随意制御（Cybernic Voluntary Control）」，②「サイバニック自律制御（Cybernic Autonomous Control）」，③「サイバニックインピーダンス制御（Cybernic Impedance Control）」，以上3つの基本機能によって，装着者が機器との一体感を得られるようになっています。

はじめに，①サイバニック随意制御について説明しましょう。人が身体を動かすとき，まず脳で「歩く」という指令が作られます。その指令は脊髄運動ニューロンを通って身体に伝わっていく。筋骨格系はその指令に反応し，当該の部位を必要なぶんだけ動かすことができます。

実は脳から神経を通じて筋骨格系に

（2面につづく）

MEMO 「希少性神経・筋難病疾患の進行抑制治療効果を得るための新たな医療機器，生体電位等で随意コントロールされた下肢装着型補助ロボット（HAL-HN01）に関する医師主導治験――短期効果としての歩行改善効果に対する無作為化比較対照クロスオーバー試験（NCY-3001試験）」（治験調整医師：中島孝）

●対象疾患：脊髄性筋萎縮症，球脊髄性筋萎縮症，下肢症状が緩徐進行性のALSなど，運動ニューロンより下位病変（詳細は，2面表＊を参照）
●2群で合計30例。主要評価項目：2分間歩行テスト，副次評価項目：10m歩行テスト・患者自身による主観的歩行評価など。その他に安全性評価
※2014年9月に追加治験として，「HTLV-1関連脊髄症（HAM）等の痙性対麻痺症による歩行不安定症に対する短期の歩行改善効果についての多施設共同無作為化比較対照並行群間治験（NCY-2001試験）」（治験調整医師：中島孝）を開始。脊髄運動ニューロンより上位病変の疾患群であるHAMなどの痙性対麻痺症に対するHAL-HN01を使った歩行プログラムの改善効果の検証を開始している。

対談 ロボットスーツHAL®は医療をどう変えるのか

＜出席者＞
●中島孝氏
1983年新潟大医学部卒。NIHフェローを経て，91年国立療養所犀潟病院，2004年より現職。専門は神経内科学，特に神経筋疾患，遺伝子診断，緩和ケア，Bioinformaticsなどの臨床研究に携わる。PMDA専門委員。厚労省難治性疾患等実用化研究事業「希少性難治性疾患――神経・筋難病疾患の進行抑制治療効果を得るための新たな医療機器，生体電位等で随意コントロールされた下肢装着型補助ロボット（HAL-HN01）に関する医師主導治験の実施研究」の研究代表者。
●川口有美子氏
1995年，母がALS（筋萎縮性側索硬化症）を発症し，介護のため英国より帰国，翌年在宅人工呼吸療法を開始。2003年，有限会社ケアサポートモモ，NPO法人ALS/MNDサポートセンターさくら会設立。04年立命館大大学院先端総合学術研究科入学。05年日本ALS協会理事，09年ALS/MND国際同盟会議理事に就任。著書には，第41回大宅壮一ノンフィクション賞を受賞した『逝かない身体』（医学書院），『末期を超えて』（青土社）。
※『末期を超えて』には中島氏との対談「QOLと緩和ケアの奪還」も掲載。

●表 歩行不安定症を起こす疾患群とHAL医療用の臨床的有用性（想定）

疾患群・病態	代表される疾患	病変のレベル	HALの臨床的有用性（想定）
神経・筋疾患＊	脊髄性筋萎縮症，筋萎縮性側索硬化症，球脊髄性筋萎縮症，筋ジストロフィー，遠位型ミオパチー，シャルコー・マリー・トゥース病など	運動ニューロンより下位の病変	有用
感染症1	ポリオ		
免疫神経疾患1	ギラン・バレー症候群，慢性炎症性脱髄性多発神経炎		
免疫神経疾患2	多発性硬化症，視神経脊髄炎	運動ニューロンより上位の病変	非常に有用
神経変性疾患	パーキンソン病関連疾患，脊髄小脳変性症，遺伝性痙性対麻痺		
脳血管障害	脳梗塞，脳内出血，くも膜下出血		
感染症2	脳炎後遺症，HTLV-1関連脊髄症		
周産期障害・先天性代謝異常症	脳性麻痺，ウィルソン病，ポンペ病		
その他の脳疾患	脳腫瘍，脳挫傷，正常圧水頭症		
脊髄障害	脊髄損傷，脊髄腫瘍，脊髄血管障害，HAM		

＊NCY-3001試験に対応

（1面よりつづく）

送られる「どの部位をどれだけ動かす」という指令は，運動単位電位（Motor Unit Potential）となり「生体電位信号」として，皮膚表面から漏れ出てきています。HALは，皮膚から出る生体電位信号をセンサから読み取り，装着者の運動意図を解釈する。そして認識した情報に即してパワーユニットをコントロールし，装着者の運動をアシストするわけです。この機能が①サイバニック随意制御に当たります。

川口 では，②「サイバニック自律制御」はどのような機能ですか。

中島 こちらは，HAL内部にあらかじめプログラムされた「起立」「歩行」などの動作パターンを参照し，HALが運動を遂行させる機能です。この機能があることで，装着者に随意運動障害がある場合でもHALがナビゲートするので，目的とする運動を成功させることができるわけです。

装着時，各関節にHALの重量がかかるのではないかとも思われますよね？ そこで機能しているのが③サイバニックインピーダンス制御で，運動時に質量と慣性モーメントに対する補正を行います。そのため，装着者はHALの荷重を意識せず，むしろ自分の身体であるかのような感覚を持って運動動作を行うことが可能になります。

川口 なるほど。それらの3機能が連動することで，難病患者さんであってもスムーズで安定した足の運びができていたわけですね。

神経筋の可塑性を促進し，「歩く力」を再獲得する

川口 すでに国内の医療・福祉施設でも，HALの下肢用は「福祉用」としてレンタルが行われ，神経・筋疾患以外の患者を対象にした歩行訓練には活用されていると聞きます。しかし，中島先生は，このHAL下肢用を「医療機器」として用いるための検証を進めてこられてきたのですよね。

中島 ええ。現在，HAL福祉用の位置付けは「福祉用具」です。そこで医療機器として扱うことができるよう，神経・筋疾患患者でも動作する医療モデルのHAL-HN01を作ってもらい，2013年3月より治験（NCY-3001試験）をスタートさせました。15年2月に治験総括報告書をまとめ，これをもってサイバーダイン社が薬事申請することになります。なお，すでに14年12月末に「希少疾病用医療機器」に指定されており，HAL医療用が優先審査などの支援措置を受けられることまで決まっているんです。

川口 ということは，HALが医療機器として使われるようになる日も，決して遠くはないことになりますね。

ただ，義足や補装具としての用途はイメージしやすいのですが，医療機器というとピンとこない患者さんも周囲には多いです。「どのような治療効果があるのか」という点が，いまいちわかりづらいのかもしれません。

中島 HALを使用することで期待される治療効果を一言で表すと，疾患によって起きる歩行不安定症（Neurologic Ambulation Disorder，表）の改善と歩行機能の再獲得に対する治療効果，そして各種疾患症状の進行抑制効果です。

川口 どんなメカニズムによってそうした効果は期待できるのでしょう。

中島 歩行不安定症を来す疾患は多種多様にありますが，麻痺が高度でなければ，シナプスネットワークの再構築が回復の手立てとなります。そのための手段としては，運動意図と，意図された運動現象の対応を繰り返し反復させる実践的な練習プログラムが有効と考えられています。

脳は，身体を動かしたとき，「どのような信号を発信し，どのように動作したのか」を確認しています。HALにアシストされながらの歩行動作であっても同様で，「歩けた」という感覚が感覚神経，脊髄を通して脳へとフィードバックされる。このように脳から運動神経を通りHALへ，HALから感覚神経，脊髄を通して脳へというインタラクティブなバイオフィードバックを正確な運動現象とともに繰り返すと，歩行の改善に向けた脳・神経・筋の可塑性を促進すると考えられているのです。

さらに神経・筋難病患者がHALを一定時間，定期的・間欠的に装着し，適切に筋収縮を助けられることで，病的筋線維の過疲労を軽減し，神経原性筋萎縮と筋力低下の進行抑制がなされるとも期待しています。

川口 それはHALを用いるからこそ可能な治療になるのですか。

中島 そう思います。人間の運動動作は単純なように見えますが，実は非常に複雑です。今，川口さんが目の前のコーヒーを口に運ぶまでの動作一つとっても，脳はとても複雑な動きをコントロールしている。

川口 肩・ひじ・手首……。いろいろな関節が複合的に動いています。

中島 歩行も同様で，左右の股関節，膝関節の複雑な多関節運動を連動し，複合的に動きます。この複雑な運動現象全体を再現し，失敗することなく反復させるためには，やはり徒手的な介入では難しく，HALのような機器が必要不可欠なのです。

もちろん「HAL単独治療」としてのみ展望しているわけではありません。将来的には抗体医薬，核酸医薬，幹細胞／iPS細胞を用いた治療と組み合わせた複合療法により，有効性をさらに高めていこうと考えています。

川口 海外ではすでにHALの医療用を実際の医療に取り入れている国もあるのだとか。

中島 早期からHALを用いた歩行プログラムを実施することで，歩行動作が改善されるという効果は国際的にも認められています。医療機器に関する品質マネジメントの規格であるISO13485は取得済みですし，それに基づいて製造された同様のモデルは，EUの医療機器に貼付が義務付けられる基準適合マークであるCEマークを13年8月に得ています。ドイツにおいては公的な労災保険に適用されているんです。

川口 すごい。HALの技術は国内を飛び越え，そこまで進んでいるんだ。

中島 14年11月にはサイバーダイン社は，HALを医療用として米国食品医薬品局（FDA）へ販売承認の申請を行いました。医療機器の大市場である米国で承認が得られることになれば，いよいよ医療ロボットが世の医療現場へ浸透していく段階に入っていくことになるでしょう。日本でも医療応用の実現化に向け，期待が高まります。

HAL・サイバニクス技術の発展にも期待が大きい

川口 実物を拝見させてもらって一番感動したのが，実はHALの技術を発展させたという「サイバニックスイッチ」でした。手指でスイッチが押せなくなったALS患者さんの腕から運動意図を拾い上げ，パソコンへの文字入力を可能にしたというのは驚きです。

中島 その技術は，HALの持つ生体電位信号から随意運動を検出する機能を独立させたデバイス「サイバニックインターフェース」が基になっています。それを応用したのが「サイバニックスイッチ」で，ALS，脊髄性筋萎縮症，筋ジストロフィー，脊髄損傷など四肢麻痺患者用の意思伝達装置に接続するための機器として開発に至りました。

川口 感度の高いスイッチを用いることで，身体を動かすことはできないほどの微弱な信号であっても，意思伝達装置を動かすことは可能になる。この技術はALS患者さんたちにとって福音です。全身性麻痺が進行する彼らにとっては，意思伝達の手段を最期まで確保できるかもしれないのですから。

中島 以前，試作機を用いて，患者さんが文章を打つ様子もご覧になっていただきましたが，川口さんにはどのように映りました？

川口 念じるだけで物を動かすことができる……。まるで『スターウォーズ』に出てくるフォースみたいだな，と（笑）。文字の打ち出しが早いので，コミュニケーションという面からのストレスも少ないと思います。

また，患者さんにかかる負担が少ないのも大事なポイントですね。従来のメカニカルスイッチでは身体のわずかな動きと力を出せる部位で操作してもらっていたわけですが，どうしても疲労の蓄積は免れなかった。1日のうちに何度もセンサを違う部位へ取り付け直し，微妙な位置合わせを行う必要がありました。でもサイバニックスイッチは筋肉を疲労させず，念じるだけです。当の患者さんも「ずっと付けてい

ても疲れないから不思議」と言っていたほどです。

早急に実用化をと思ってしまうのですが，こちらはまだ時間がかかりそうですか。

中島　まだ製品化に向けて準備を進めてもらっている段階です。製品化された上で，定期的・間欠的に利用することで，ALSをはじめとした疾患の進行抑制が期待できるかどうかも検証したいと思っています。

HALによる臨床的効果を患者の主観で評価

川口　治験では，副次評価項目に「患者自身による主観的歩行評価」を取り入れられていますね。患者さんの思いを評価し，その変化に着目している点はユニークだなと感じていたんです。

中島　HALを用いた治療プログラムを通し，患者さんがいかに疾患・障害を持つ生活に適応できるようになったのかを計量的に評価したいという思いから，患者さんの報告するアウトカム（Patient Reported Outcome；PRO）を副次評価項目に入れました。

ただ，医療者にも誤解されがちなのですが，そもそもQOLはPROのひとつであって，患者の心の中に作られる知覚・意味といった「構成概念」です。その内容の改善こそがQOLの改善を意味するわけですから，本来ならばあらゆる治療介入の最終目標にPROを据えるべきなのです。

川口　今回，PROとして難病・障害患者さんのQOL評価を行ったのは，適切にQOLを評価できるからということですね。

中島　ええ。PROとしてのQOLの評価は，難病などで治癒をめざせず，進行性に悪化する患者に対する介入・ケアの効果を評価する場合には特に有効です。他の評価法と比較しても，より適切な評価が可能だと思います。

川口　しかし，どうして他の評価法では不十分なのでしょうか。

中島　医療現場でよく見掛ける評価尺度として，WHOの健康概念に基づいた健康関連QOL評価法，例えばEuro-QoL（EQ-5D）やThe Medical Outcome Study 36-Item Short Form Health Survey（SF-36）があります。しかし，これらの評価尺度で難病患者・家族のQOLの改善効果を評価するのは難しい。というのも，それらはWHO憲章前文が定義した「健康」の概念が前提となっており，その文言は「complete physical, mental and social well-being」，つまり身体的，心理的，社会的に完全に良い状態こそが「健康である」としているからです。

川口　確かにそれが「健康」の基準になってしまうと，治癒を望めない難病や障害を持つ方，または身体機能が加齢とともに落ちる高齢者は，「健康」になり得なくなってしまいます。

中島　そうなのです。WHOの言う「健康」の定義に向かって改善し得ない彼らは，健康関連QOL評価法によっては，QOLの改善を適切に評価することができない。評価する生活領域が固定されていることを考えると，むしろ現状の患者・家族にとって無関係となってしまった生活領域を，解決できない問題としていたずらに顕在化させることすらある。これでは難病の患者・家族に，「疾患により起きる問題」だけでなく，「文化的・社会的文脈に内在する健康志向的価値観に由来する自己否定感」という二重の困難を与えてしまいます。

また，治療・ケアに当たる医療従事者を無力感で苦しませる可能性もありますし，「治癒できない，健康に戻れない患者」として，「支援すべき患者」を否定してしまう事態まで起こりかねません。

川口　実際に難病患者・家族と接すればわかることですが，皆さん，いわゆる「残存している機能」を活かすことで，QOLを高めていくことができていますよね。そこは医療者の方々には誤解してほしくない部分です。

中島先生は今回の治験でPROを導入するに当たり，具体的にはどのような方法を採用されたのでしょうか。

中島　SEIQoLという方法です。SEIQoLは，評価項目の構成を対象となる患者自身に任せます。つまり患者自身の人生において，大切に思っていることがうまくいったり，満足したりすることをQOLの向上と定義し，QOLの項目として本人にとって大切な生活分野を5つ構成してもらって調査がスタートする（註）。こうすると個人別のQOL評価が可能になるわけです。

細かな方法論は割愛しますが，経時的に生活領域が変化していっても適用可能であり，計量心理学的にも正しい方法として評価が可能です。

価値観，意味の再構成により，人は難病・障害を克服できる

川口　患者さんの主観を評価するとなると「いい加減だ」「科学的でない」と思われてしまう面もあるのではないですか。本来，そのいい加減さこそが患者さんの，人間としての実像であるにもかかわらず，ですけれど。

中島　これまでPROの研究が進んでこなかったのも，やはり患者の主観が「いい加減で，扱いづらいもの」として見られていた面があったからなのでしょう。

実際に主観的評価を採用してみると，やはり人は時間経過によって，評価尺度自体を変える「recalibration」，価値判断の優先順位を変える「reprioritization」や，言葉の意味や内容を変える「reframe」を起こし，同じ事象に対しても評価を変えるレスポンスシフト（response shift）現象を起こしていることがわかっています。ですから主観により臨床効果を評価する上では，そうした現象を理解し，考慮する必要があるのは間違いありません。

ただ，川口さんのご指摘のとおりで，これは人間にとって当然の現象です。レスポンスシフトは単に患者の記憶があいまいで，いい加減だから起こるものではない。患者が事象に対する構成概念を書き換える，つまり，その人の心の中に，これまでとは異なった価値観・意味が再構成されることで起こっているものなのです。

確かにとらえづらく，評価の難しさはありますが，その中には治癒し得ない難病という問題に適応し，自ら管理しようと蘇ってくる患者さんの力がある。PROはそれを見ることに対応していると言えます。

川口　人はどんな状況にあっても，考え方，価値観を変化させ，自分の生きやすいストーリーに作り変えていくポテンシャルを持っていますよね。

中島　そう。だから，医療者は治療やケアにより身体的な状態が良くなったかどうかだけではなく，治療によって患者にどのようなレスポンスシフトが起きたのかをきちんと評価すべきであると，私は考えているんです。

事象に対する構成概念を書き換えていく能力，それは難病・障害を克服する力にもなります。この力の在りようを見て，減弱していれば，きちんと支援を行う。時に医薬品・医療機器を使いながら，患者さんの心と身体を蘇らせ，生きることを支援する。それこそが医療の真の姿なのですから。

川口　冒頭，HALを使うと患者さんが笑顔になることに触れました。これはHALが心と身体を支え，患者さんの構成概念の書き換えに何らかの好影響を与えているからなのでしょうね。

中島　そう考えています。ですから今回のHALの治験でも，治療プログラムを経て，患者さんが主観をどのように変遷させてきたのかを経時的に追ってみようとしています。うまくいくかはわかりませんが，真に患者さんのためになる治療モデルを作る試みと言えるのかもしれません。

難病研究が技術革新の最前線を担う

中島　歴史を振り返ると，技術革新は戦争という極限状態によってもたらされたと言われることがありますよね。しかし，現代社会において技術革新の最前線を担うのは難病研究である，というのが私の考えです。だってそうでしょう？　ALSや筋ジストロフィー患者さんが利用できるロボットスーツを作り上げたとしたら，それは軍事目的で作られるロボットよりも高性能に違いありません。

川口　屈強な兵士を対象としたものより，多様なサポートを必要する難病患者対象のロボットスーツのほうが，安全性も含めて高度な技術が求められそうですものね。

中島　さらに言えば，現在進めているHALの研究は，高齢者への適用も射程に入れています。患者数の少ない難病に対する研究として日本から始まったものではありますが，高齢者医療における治療法開発という国際的な共通課題に立ち向かう研究とも言えるわけです。そういう意味でも，HALの研究に叡智を結集する意義は大きいと考えています。

日本においてこの技術の進化を進めていくことができれば，それは国境を越え，世界の人々をも助けるものになる。それは日本の国際的な信頼獲得につながるでしょうし，今後，経済的な好影響も伴うはずです。

川口　根治困難な疾患・障害を対象とした日本の研究が，科学技術，さらに社会の進展の原動力になるということになりますね。いずれ難病研究が“ジャパニーズ・クール”なものとして世界から注目されるのかもしれません。

その貴重な第一歩として，HALの医療現場への活用を期待したいと思います。ありがとうございました。

（了）

註：SEIQoL（The Schedule for Evaluation of Individual QoL）。半構造化面接法によって，患者自身が自分にとって大切と考えている生活の領域を5つ引き出し，患者自身にその内容を定義し，名付けてもらう。そして，それぞれの生活領域がどの程度うまくいっているのか，満足しているのかを視覚アナログスケールにより評価。さらに5つの領域がその人の生活においてどのような重みで意識されているのかを計測する。重みを計測するためには判断分析法という多変量解析を利用する。重み付けすることで，一元的なQOL（SEIQoL-indexスコア）が算出できる。臨床場面では，より簡易な方法としてSEIQoL-DWが利用されることが多い。
日本語版SEQoLウェブサイト
http://seiqol.jp

●参考文献
1）中島孝．神経・筋難病患者が装着するロボットスーツHALの医学応用に向けた進歩，期待される臨床効果．保健医療科学．2011；60（2）：130-7.
2）中島孝．医療におけるQOLと緩和についての誤解を解くために．医薬ジャーナル．2011；47（4）：1167-74.
3）中島孝，他．装着型ロボット応用の現状と展望．治療．2013；95（12）：2088-93.
4）中島孝．ロボットスーツ“HAL-HN01（医療用HAL）”．医学のあゆみ．2014；249（5）：491-2.
5）中島孝．難病の画期的治療法，HAL-HN01の開発における哲学的転回．現代思想．2014；42（13）：137-45.
6）中島孝．神経難病患者の生活の質評価．作業療法ジャーナル．2015；49（1）：14-9.

ELSEVIER

CrossMark

The Spine Journal 14 (2014) 2847–2853

THE SPINE JOURNAL

Clinical Study

Voluntary driven exoskeleton as a new tool for rehabilitation in chronic spinal cord injury: a pilot study

Mirko Aach, MD[a,*], Oliver Cruciger, MD[a], Matthias Sczesny-Kaiser, MD[b], Oliver Höffken, MD[b], Renate Ch. Meindl, MD[a], Martin Tegenthoff, MD[b], Peter Schwenkreis, MD[b], Yoshiyuki Sankai, PhD[c], Thomas A. Schildhauer, MD[d]

[a]*Department of Spinal Cord Injuries, BG University Hospital Bergmannsheil, Bürkle-de-la-Camp-Platz 1, 44797, Bochum, Germany*
[b]*Department of Neurology, BG University Hospital Bergmannsheil, Bürkle-de-la-Camp-Platz 1, 44797, Bochum, Germany*
[c]*Faculty of Engineering, Information and Systems, University of Tsukuba, 1-1-1 Tennodai, Tsukuba, Ibaraki 305-0006, Japan*
[d]*Department of General and Trauma Surgery, BG University Hospital Bergmannsheil, Bürkle-de-la-Camp-Platz 1, 44797, Bochum, Germany*

Received 17 December 2013; revised 20 March 2014; accepted 28 March 2014

Abstract

BACKGROUND CONTEXT: Treadmill training after traumatic spinal cord injury (SCI) has become an established therapy to improve walking capabilities. The hybrid assistive limb (HAL) exoskeleton has been developed to support motor function and is tailored to the patients' voluntary drive.

PURPOSE: To determine whether locomotor training with the exoskeleton HAL is safe and can increase functional mobility in chronic paraplegic patients after SCI.

DESIGN: A single case experimental A-B (pre-post) design study by repeated assessments of the same patients. The subjects performed 90 days (five times per week) of HAL exoskeleton body weight supported treadmill training with variable gait speed and body weight support.

PATIENT SAMPLE: Eight patients with chronic SCI classified by the American Spinal Injury Association (ASIA) Impairment Scale (AIS) consisting of ASIA A (zones of partial preservation [ZPP] L3–S1), n=4; ASIA B (with motor ZPP L3–S1), n=1; and ASIA C/D, n=3, who received full rehabilitation in the acute and subacute phases of SCI.

OUTCOME MEASURES: Functional measures included treadmill-associated walking distance, speed, and time, with additional analysis of functional improvements using the 10-m walk test (10MWT), timed-up and go test (TUG test), 6-minute walk test (6MWT), and the walking index for SCI II (WISCI II) score. Secondary physiologic measures including the AIS with the lower extremity motor score (LEMS), the spinal spasticity (Ashworth scale), and the lower extremity circumferences.

FDA device/drug status: Not applicable.

Author disclosures: ***MA:*** Nothing to disclose. ***OC:*** Nothing to disclose. ***MS-K:*** Nothing to disclose. ***OH:*** Nothing to disclose. ***RCM:*** Nothing to disclose. ***MT:*** Nothing to disclose. ***PS:*** Nothing to disclose. ***YS:*** Royalties: University of Tsukuba (E); Stock Ownership (E, Paid directly to institution); Private Investments: (E, Paid directly to institution); Consulting: (E, Paid directly to institution); Speaking / Teaching Arrangements: (E, Paid directly to institution); Trips/Travel: (E, Paid directly to institution); Board of Directors: CYBERDYNE, Inc. (E); Grants: Cabinet Office (I). ***TAS:*** Nothing to disclose.

The disclosure key can be found on the Table of Contents and at www.TheSpineJournalOnline.com.

There has been no monetary study funding. The study was supported by a grant and has been supervised by the staff of BG University Hospital Bergmannsheil, Bochum.

Authors' contributions: MA and OC carried out the experiments and data analysis as well as drafting of the manuscript. RCM, PS and MT helped with the experimental set up. MS-K and OH contributed to the data analysis. TAS participated in study design and coordination of the study.

All authors read and approved the final manuscript.

YS is a founder, shareholder, and the CEO of Cyberdyne, Inc., which produces the HAL.

YS and Cyberdyne were neither involved in study funding, design, data collection, and analysis, nor in writing or submitting this article, therefore concluding in no specific influence on the trial. We certify that no party having a direct interest in the results of the research supporting this article has or will confer a benefit on us or on any organization with which we are associated.

YS and Cyberdyne as the manufacturer of the device provided exclusively technical and advisory support.

YS as the CEO of Cyberdyne has been involved exclusively in terms of an advisory capacity, regarding technical support and the limitations of the exoskeleton. Therefore, the inclusion and exclusion criteria have been modified (eg, body weight and contractures).

* Corresponding author. Department of Spinal Cord Injuries, BG University Hospital Bergmannsheil, Bürkle-de-la-Camp-Platz 1/44789, Bochum, Germany. Tel.: 81 29-853-2111.

E-mail address: bergmannsheil@bergmannsheil.de (M. Aach)

1529-9430/$ - see front matter
http://dx.doi.org/10.1016/j.spinee.2014.03.042

METHODS: Subjects performed standardized functional testing before and after the 90 days of intervention.

RESULTS: Highly significant improvements of HAL-associated walking time, distance, and speed were noticed. Furthermore, significant improvements have been especially shown in the functional abilities without the exoskeleton for over-ground walking obtained in the 6MWT, TUG test, and the 10MWT, including an increase in the WISCI II score of three patients. Muscle strength (LEMS) increased in all patients accompanied by a gain of the lower limb circumferences. A conversion in the AIS was ascertained in one patient (ASIA B to ASIA C). One patient reported a decrease of spinal spasticity.

CONCLUSIONS: Hybrid assistive limb exoskeleton training results in improved over-ground walking and leads to the assumption of a beneficial effect on ambulatory mobility. However, evaluation in larger clinical trials is required.

Keywords: Exoskeleton; Treadmill training; Rehabilitation; Paraplegia; Hybrid assistive limb; Spinal cord injury

Introduction

About 1,200 people suffer a traumatic spinal cord injury (SCI) each year in Germany. Recent statistics indicate that more than 50% of these injured patients have a motor incomplete lesion [1]. In patients with initial motor incomplete SCI, at least 75% regain some kind of ambulatory function. Better functional outcome is associated with age, level of lesion, and the classification in the American Spinal Injury Association (ASIA) Impairment Scale [2]. In the first 2 months after initial SCI, approximately half of the recovery occurs. Within the following 4 months, a decreasing rate of recovery has been observed. One year after injury, neurologic recovery is assumed to be nearly complete [3]. Although conventional rehabilitation programs enhance the performance of functional tasks, the loss of strength and coordination substantially limit one's capacity for over-ground ambulation training [4]. In the past two decades, body weight supported treadmill training (BWSTT) has been proposed as a useful adjunct to enhance locomotor function after motor incomplete SCI [5]. In patients with incomplete or complete SCI, a bilateral leg muscle activation combined with coordinated stepping movements can be induced in partially unloaded patients, standing on a moving treadmill. Body weight supported treadmill training enables early initiation of gait training and integration of weight-bearing activities, stepping and balance, by the use of a task-specific approach and a systematic gait pattern [6]. To facilitate the delivery of BWSTT in SCI patients, the locomotor training evolved over the last 12 years and a motorized robotic driven gait orthosis (DGO) has been developed [7]. The advantages over conventional BWSTT methods are considered to be less effort for attending physiotherapists [8], longer duration, more physiologic and reproducible gait patterns, and the possibility to measure a patients' performance. Several studies pointed out that DGO training improves over-ground walking [9–13]. However, there was no reported difference in the outcome of DGO training compared with conventional training. A significant switch in the ASIA classification has not been found [10,14].

Over the last 5 years, exoskeletal systems became available for SCI patients. These systems offer different possibilities. Three exoskeletons (Ekso [EksoBionics, Richmond, CA, USA], Rex [Rex Bionics, Aukland, New Zealand] and Re-Walk [ARGO Medical Technolgies, Israel]) allow SCI patients to stand up, walk with a defined pattern, and even climbing stairs mainly on a basis of passive range of motion (ROM). The exoskeleton hybrid assistive limb (HAL; Cyberdyne, Inc., Japan) offers the possibility of getting connected with the SCI patient through electromyography electrodes on the skin at the extensor/flexor muscle region of the lower extremities. This allows voluntary machine supported ROM of incomplete SCI patients by using minimal bioelectrical signals, recorded and amplified from hip and knee flexors and extensors [15–17]. More recently, these various exoskeletal systems allow the patients mobilization outside the treadmill. A former study by Kawamoto et al. [18] concerning locomotion improvement using HAL in chronic stroke patients, emphasized the feasibility for rehabilitation of these particular patients.

The aim of this pilot study was to evaluate the possibilities of exoskeletal locomotor training (HAL; Cyberdyne, Inc.) under voluntary control and identify beneficial effects on functional mobility of the patients. The hypothesis was that exoskeleton treadmill training is feasible and safe in application and capable of improving ambulatory mobility in chronic SCI patients.

Materials and methods

Patients

We enrolled eight patients (two women, six men). The mean±standard deviation age at the time of enrollment was 48±9.43 years. All patients were in the chronic stage of traumatic SCI according to the time since injury of 1 to 19 years (97.2±88.4 months). Inclusion criteria were traumatic SCI with chronic incomplete (ASIA B/C/D) or complete paraplegia (ASIA A) after lesions of the conus medullaris/cauda equine with zones of partial preservation. Independent of ASIA classification, the enrolled patients

must present motor functions of hip and knee extensor and flexor muscle groups to be able to trigger the exoskeleton. Exclusion criteria were as follows: nontraumatic SCI, pressure sores, severe limitation of ROM regarding hip and knee joints, cognitive impairment, body weight more than 100 Kg, nonconsolidated fractures, and mild or severe heart insufficiency. Two patients suffered from an incomplete thoracic SCI (ASIA C/D) from 3 to 13 years. Two patients suffered from an incomplete lumbar SCI (ASIA B/C) from 12 to 13 months and four patients had a complete SCI with zones of partial preservation in L3–S1 after lesions of the conus medullaris. The classification according to the ASIA was carried out before the treadmill training was initiated. The study was approved by Ethical Board Committee of Bergmannsheil Hospital and the University of Bochum and followed strictly the declaration of Helsinki.

All patients provided written informed consent. The study design was a single case experimental A-B (pre-post) design by repeated assessments of the same patients (Table 1).

Intervention

During this study, the patients underwent a BWSTT five times per week using the HAL exoskeleton (Cyberdyne, Inc., Japan). The study was performed between June 2013 and September 2013 in the BG University Hospital Bergmannsheil, Bochum.

Neither adverse nor severe adverse events occurred during the intervention.

The exoskeleton

The HAL robot suit (Cyberdyne, Inc., Japan) is an exoskeleton with a frame and robotic actuators that attach to the patients' legs. The joint movement is supported by electric motors. Voluntary initiated minimal bioelectrical signals recovered from extensor and flexor muscles of hip and knee are detected via electromyography electrodes (Fig. 1).

Through a cable connection between the exoskeleton and patient, this system allows voluntary robotic supported ROM (cybernic voluntary control mode). Also a passive, nonvoluntary ROM (cybernic autonomous control mode) is possible (Fig. 2).

The treadmill

The treadmill system (Woodway USA, Inc., Waukesha, WI, USA) includes a body weight support system with a harness. The speed can be adjusted from 0 Km/h to approximately 4.5 Km/h. During treatments, the velocity of the treadmill was set individually between comfortable and maximum speed tolerated by the patients. Approximately 50% of each patient's body weight needed to be supported by the harness system, individually reduced during the following sessions as tolerated without substantial knee buckling or toe drag.

EVIDENCE & METHODS

Context
The authors present a series of patients treated with an assistive exoskeleton developed to facilitate treadmill exercise in patients with spinal cord injury (SCI).

Contribution
In a series of eight patients with SCI graded ASIA A to C/D, improvements in walking time, distance and speed were noted after treatment with assistive exoskeleton.

Implications
This study is a case series of eight patients with heterogeneous clinical characteristics, including the severity of their spinal cord injury. The findings are limited to clinical contexts specific to these patients and clearly cannot be translated to the care of other individuals. This is simply a report that may show proof of concept. It should be noted that one of the authors reports a substantive conflict of interest (founder and shareholder of the company that produces the exoskeleton device).

—The Editors

The training

The patients underwent a 90-day period of HAL exoskeleton (Cyberdyne, Inc.) training (five per week), including a mean number of sessions of 51.75±5.6. The training was performed on a treadmill with individually adjustable body weight support and speed, recording walking speed, time, and distance. It included a 10-m walk test (10MWT) before and after each session and regular physiotherapy that lasted approximately 90 minutes. The training was supervised by a physiotherapist and a medical doctor.

Measurements

Walking capabilities and neurologic status

All patients were assessed on admission by medical doctors involved in this trial. The outcomes were assessed

Table 1
Subject demographics and clinical characteristics

Case	Sex	Age (y)	Time since trauma, y	Etiology	Level	ASIA/ZPP	WISCI II	Ashworth
1	M	40	13	# T7/T8	T8	C	13	4
2	M	63	1	# T12	L1	B/L3	6	0
3	M	36	1.16	# T11/T12	T12	A/L3	6	0
4	F	55	1.08	# L1	L1	C	13	0
5	M	42	16	# L1	L1	A/L3	9	0
6	M	52	10	# L3	L2	A/L3	6	0
7	F	40	19	# L1	T11	A/S1	9	0
8	M	53	3	# T12	T12	D	18	0

M, male; F, female; #, fracture; ASIA, American Spinal Injury Association; ZPP, zones of partial preservation; WISCI, walking index for spinal cord injury; T, thoracic; L, lumbal; S, sacral.

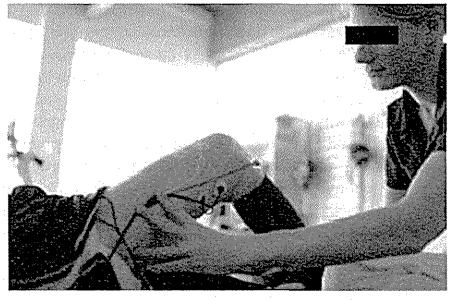

Fig. 1. Positioning of the electromyography electrodes on the knee extensor and flexor muscles.

by physiotherapists neither involved in the study design nor analysis after 45 days and on discharge from the training period. An assessment through the ASIA classification

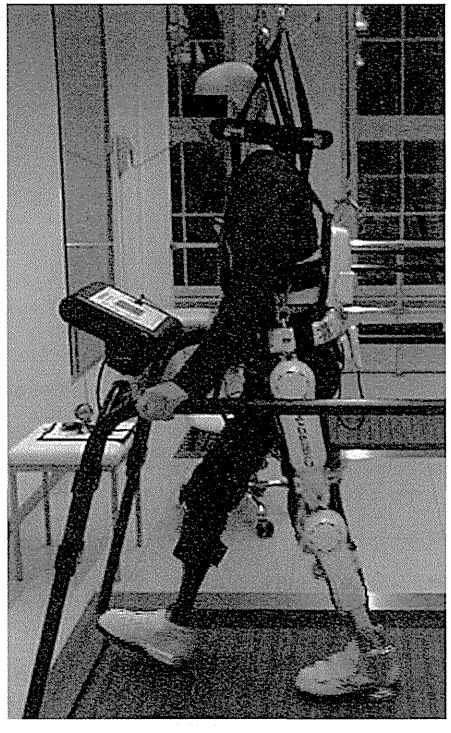

Fig. 2. Patient performing treadmill locomotion training with body weight support and hybrid assistive limb exoskeleton.

was already done on admission and on discharge from the SCI department, Bergmannsheil, Bochum, within the initial therapy after acute SCI. The 10MWT, done before and after each session, detected the needed time, the number of steps, and the required assistance to walk a 10 m distance [19,20]. The timed-up and go test (TUG test) describes the time and assistance required for standing up from the wheelchair, walk 3 m, turn around, walk back, and sit down. It was performed every 2 weeks. The 6-minute walk test (6MWT) was done at the beginning, at half time, and at the end if possible, depending on the patient. It evaluates the distance and assistance while walking for 6 minutes [21]. The main outcome was the functional motor assessment by the walking index for SCI II (WISCI II) [22,23]. The WISCI II score is a 20-item scale, measuring the walking capabilities of a patient based on the requirements of assistance because of walking aids, personal assistance, or braces. Grade 0 means that the patient has neither standing nor walking abilities. Grade 20 means that no assistance is needed to walk a distance of 10 m. The neurologic status was assessed using the ASIA Impairment Scale modified from the Frankel classification and classifies motor and sensory impairments that result from a SCI [3]. The lower extremity motor score (LEMS) acquired in this study was obtained by the addition of the impairment scores (0–5) of the lower extremity key muscles of both sides. Muscle volume was assessed by manual measurements, 20/10 cm above and 15 cm below inner knee gap.

Statistical analysis

Descriptive analysis of the demographic and injury characteristics was done using frequency distribution for categorical data and mean for continuous variables. Differences between pre- and posttraining sessions were assessed by a paired *t* test (for continuous variables). Treatment effects on functional performance as the WISCI II are all ordinal scales. Medians were used as descriptive statistics for these outcomes, and nonparametric tests were used to assess the relative effect of the treatments.

Results were considered statistically significant when the p value was ≤.05.

Results

Treadmill associated results

All patients improved in treadmill training by using HAL (Cyberdyne, Inc., Japan). The mean walking speed increased from 0.91±0.41 m/s (0.5–1.8 m/s) in the first session up to 1.59±0.5 m/s (0.8–2.1 m/s) in the last session after 3 months. The progress in speed after 6 weeks of training was lower than in the first weeks. The range was located between 0 km/h and 0.8 km/h. The mean walking time at the beginning was 12.37±4.55 minutes. The average walking time at the

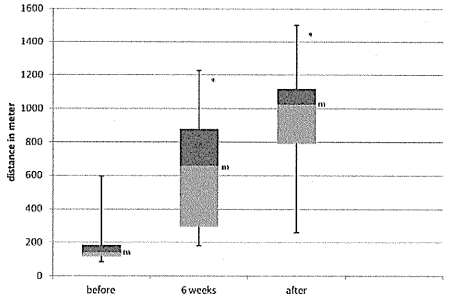

Fig. 3. Changes in treadmill-associated walking distance in pre-, mid-, and postevaluations. m, median. *pre-post difference, p<.05.

end was 31.97±9.45 minutes. The mean ambulated distance at the first session was 195.9±166.7 m and increased to 954.13±380.4 m on discharge (Fig. 3).

Functional outcome

Although the mean improvement concerning the WISCI II score was not statistically significant, three patients showed functional improvement in gait abilities. Two subjects needed braces, a walker, and support by a physiotherapist at the beginning and were able to walk after the training series only with a walker and braces (WISCI II score increased from 6 to 9). One patient increased from 9 to 12 and, therefore, was able to walk with two crutches and a brace compared with a walker and a brace before the training. At baseline, the mean WISCI II score was 10±4.3. At the end of the 90 days trial, the mean WISCI II was 11.13±6.68. Improvements in speed and endurance in over-ground gait assessments in all participants have been achieved. The 10MWT showed a significant increase in mean gait speed at the end of the training period compared with baseline (0.28±0.28 m/s vs. 0.50±0.34 m/s) (Fig. 4).

The improvement corresponded to a 44% faster walking than in initial evaluation. It also includes the reduction of

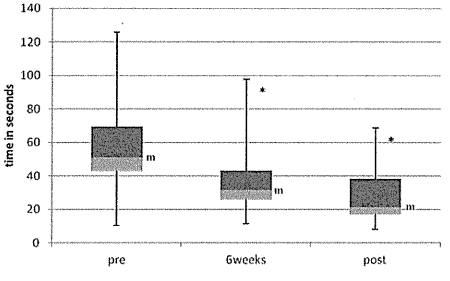

Fig. 4. Changes in 10-m walk test in pre-, mid-, and postintervention evaluations. m, median. *pre-post difference, p<.05.

Table 2
Comparison of pre- and postinterventions

Outcome measurements	Before training	After training	n
10MWT speed (m/s)	0.28±0.28	0.5±0.34*	8
Number of steps	29.88±7.85	19.38±3.16*	8
6MWT distance (m)	70.1±130	163.3±160.6*	8
TUG test (s)	55.34±32.20	38.18±25.98*	8
Distance (m)	195.88±166.71	954.13±380.35*	8
WISCI-II	10±4.34	11.12±3.68	8

10MWT, 10-m walk test; 6MWT, 6-minute walk test; TUG, timed-up and go; WISCI, walking index for spinal cord injury.
Note: Values are means±standard deviation.
* Pre-post difference, p<.05.

support needed detected by the WISCI II score. The mean number of steps decreased from 29.8±7.85 to 19.4±3.16. We observed significant increase in gait speed from pre- to midtraining and from mid- to posttraining assessments. Similar results were detected for the TUG test. The mean time needed for the TUG test decreased from 55.34±32.2 seconds to 38.18±25.98 seconds. The 6MWT was done with a constant walking time of 6 minutes without any break. Only three patients were able to perform the 6MWT before the training with a mean walking distance of 187±162.2 m. The subjects in this subgroup improved their performance and increased the walking distance to 287.3±229.4 m. After completing the training, all eight patients could be evaluated, therefore the overall mean distance increased from 70.1±130 m to 163.3±160.6 m (Table 2).

The LEMS increased in all patients. The mean LEMS before the training increased significantly from 21.75±8.3 to 24.38±7.6 after the intervention (Fig. 5).

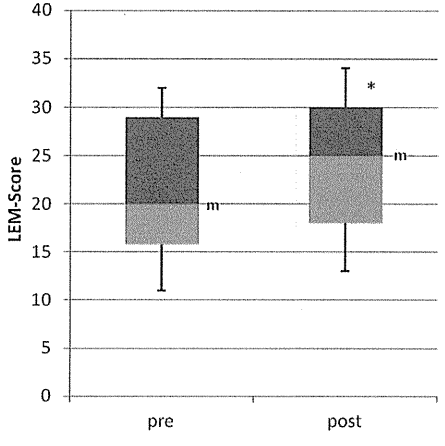

Fig. 5. LEMS in pre- and postevaluation. LEM, lower extremity motor score; m, median. *pre-post difference, p<.05.

One patient switched in the ASIA scale from ASIA B to C, he was at the beginning of the training 12 months posttrauma.

Others

To describe muscle volume, measurements of the circumferences 10/20 cm cranial of the inner knee joint gap and 15 cm distal of it have been done before and after the 90 days of training. Seven participants showed a gain of muscle circumference from 5 mm up to 50 mm. In one participant with edema in his lower legs, we observed a loss of circumference up to 25 mm. One patient suffering from a thoracic SCI presented a significant spinal spasticity. For spastic motor behaviors, we used the modified Ashworth scale to evaluate the involuntary resistance to passive stretch of the quadriceps muscle group. At pretraining evaluation, he showed an extensor spasm with high resistance to passive stretch according to Ashworth 4. After the training sessions, the resistance was reduced according to Ashworth 2. This level lasted for about 6 to 8 hours with a new maximum level at the next morning. All other patients showed no spastic motor behaviors.

Discussion

The objective of the study was to determine whether locomotor training with the exoskeleton HAL is feasible and safe in application, improves functional mobility, and increases motor functions in chronic paraplegic patients after SCI. The results obtained revealed a highly significant improvement for over-ground walking abilities evaluated by the 10MWT, the 6MWT, and the TUG test and the partial reduction of physical assistance and walking aids in the WISCI II score. Muscle strength, measured with the LEMS increased in all patients.

The results acquired in this clinical trial imply that HAL-supported locomotion training can improve walking abilities in terms of speed, gait, and distance. Furthermore, it improves motor functions.

Thus far there is insufficient evidence and only a few articles addressing the main hypothesis of this study that locomotor training improves walking function for patients with SCI [24].

The present study is according to the knowledge of the authors the first to investigate the impact of HAL-supported locomotor training in chronic SCI patients, where referring to the current state of knowledge no further functional improvements are to be expected.

In the subject population consisting of eight patients including patients suffering from SCI from 1 to 19 years (8.03±7.4 years), all patients improved significantly regarding treadmill-associated walking distance and speed and functional improvement was detected in the over-ground walking tests.

Although no significant influence was seen on the requirements of assistance in the 10MWT, three patients attained improvement in walking abilities according to the WISCI II, under condition of a comfortable and stable gait. A further reduction of assistance was not forced because of more pathologic gait or higher risk of falling [24].

Although the evidence is still insufficient, the effectiveness of automated locomotor training using the DGO in patients with chronic SCI is being investigated and considered promising in several systematic reviews including a Cochrane review [25,26]. The results mentioned previously add to the wealth of that data presuming that HAL-assisted locomotion training is useful in terms of functional mobility and a safe adjunct to the treatment of patient with chronic SCI.

Our study had several limitations: the relatively small number of patients (n=8) and the mixture of complete and incomplete SCIs.

However, all the patients were treated in the same facility by the same multidisciplinary team, according to a standardized protocol.

In summary, our study provides the first data demonstrating the clinical potential of HAL-locomotor training based on voluntary drive in patients suffering from chronic SCI.

It was proven to be a safe device for locomotion therapy as neither adverse nor severe adverse events occurred.

However, continued research in the form of large randomized trials to compare the efficacy of HAL-assisted training with well established, conventional therapies is necessary.

References

[1] Eng J, Teasell R, Miller W, et al. Spinal cord injury rehabilitation evidence: methods of the SCIRE systematic review. Top Spinal Cord Inj Rehabil 2007:13:1–10.
[2] Waters RL, Adkins R, Yakura J, Vigil D. Prediction of ambulatory performance based on motor scores derived from standards of the American Spinal Injury Association. Arch Phys Med Rehabil 1994;75:756–60.
[3] Piepmeier JM, Jenkins NR. Late neurological changes following traumatic spinal cord injury. J Neurosurg 1988:69:399–402.
[4] Gittler MS, McKinley WO, Stiens SA, et al. Spinal cord injury medicine. 3. Rehabilitation outcomes. Arch Phys Med Rehabil 2002;83:S65–71.
[5] Finch L, Barbeau H, Arsenault B. Influence of body weight support on normal human gait: development of a gait retraining strategy. Phys Ther 1991:71:842–55; discussion 855–6.
[6] Dietz V, Wirz M, Curt A, Colombo G. Locomotor pattern in paraplegic patients: training effects and recovery of spinal cord function. Spinal Cord 1998;36:380–90.
[7] Colombo G, Joerg M, Schreier R, Dietz V. Treadmill training of paraplegic patients with a robotic orthosis. J Rehabil Res Dev 2000;37:693–700.
[8] Winchester P, Querry R. Robotic orthosis for body weight-supported treadmill training. Phys Med Rehabil Clin N Am 2006:17:159–72.
[9] Colombo G, Wirz M, Dietz V. Driven gait orthosis for improvement of locomotor training in paraplegic patients. Spinal Cord 2001:39: 252–5.
[10] Wirz M, Zemon DH, Rupp R, et al. Effectiveness of automated locomotor training in patients with chronic incomplete spinal cord

injury: a multicenter trial. Arch Phys Med Rehabil 2005;86: 672–80.
[11] Hornby TG, Zemon DH, Campbell D. Robotic assisted, body-weight-supported treadmill training in individuals following motor incomplete spinal cord injury. Phys Ther 2005;85:52–66.
[12] Hornby TG, Campbell DD, Zemon DH, Kahn JH. Clinical and quantitative evaluation of robotic-assisted treadmill walking to retrain ambulation following spinal cord injury. Top Spinal Cord Inj Rehabil 2005;11:1–17.
[13] Nooijen CF, Ter Hoeve N, Field-Fote EC. Gait quality is improved by locomotor training in individuals with SCI regardless of training approach. J Neuroeng Rehabil 2009;6:36–46.
[14] Schwartz I, Sajina A, Neeb M, et al. Locomotor training using a robotic device in patients with subacute spinal cord injury. Spinal Cord 2011;49:1062–7.
[15] Kawamoto H, Sankai Y. Power assist system HAL-3 for gait disorder person. Proceedings of ICCHP international conference on computers helping people with special needs. 2002; 196–203.
[16] Suzuki K, Mito G, Kawamoto H, et al. Intention-based walking support for paraplegia patients with robot suit hal. Advanced Robotics 2007;21:383–408.
[17] Yamawaki K, Kawamoto H, Eguchi K, et al. Gait training for a spinal canal stenosis patient using robot suit HAL: a case report-. Proceedings of the 6th World Congress of the International Society of Physical and Rehabilitation Medicine, 2011; 66–68.
[18] Kawamoto H, Kiyotaka K, Yoshio N, et al. Pilot study of locomotion improvement using hybrid assistive limb in chronic stroke patients. BMC Neurol 2013;13:141.
[19] Van Hedel HJ, Wirz M, Curt A. Improving walking assessment in subjects with an incomplete spinal cord injury: responsiveness. Spinal Cord 2006;44:352–6.
[20] Van Hedel HJ, Wirz M, Dietz V. Assessing walking ability in subjects with spinal cord injury: validity and reliability of 3 walking tests. Arch Phys Med Rehabil 2005;86:190–6.
[21] Harada ND, Chiu V, Stewart AL. Mobility-related function in older adults: assessment with a 6-minute walk test. Arch Phys Med Rehabil 1999;80:837–84.
[22] Ditunno JF, Ditunno PL. Walking index for spinal cord injury (WISCI II): scale revision. Spinal Cord 2001;39:654–6.
[23] Myeong OK, Burns AS, Ditunno JF, Marino RJ. The assessment of walking capacity using the walking index for spinal cord injury: self-selected versus maximal levels. Arch Phys Med Rehabil 2007;88:762–7.
[24] Nascimento LR, Caetan LC, Freitas DC, et al. Different instructions during the ten-meter walking test determined significant increases in maximum gait speed in individuals with chronic hemiparesis. Rev Bras Fisioter 2012;16:122–7.
[25] Mehrholz J, Kugler J, Pohl M. Locomotor training for walking after spinal cord injury. Cochrane Database Syst Rev 2012;11.
[26] Morawietz C, Moffat F. Effects of locomotor training after incomplete spinal cord injury: a systematic review. Arch Phys Med Rehabil 2013;94:2297–308.

Development of an MR-compatible Configurable Brush Stimulation Device

K. Murata-*Student Member*, A. Matsushita-*IEEE Member*, K. Saotome, H. Kawamoto, and Y. Sankai-*IEEE Member*

Abstract— **In order to evaluate sensory disturbance, a subjective method is performed, so that the evaluation result is influenced by subjective factors. fMRI is used for observing brain activity objectively. Therefore the brain response to a stimulation measured by fMRI could become a useful identification tool for the objective evaluation. The purpose of this study is to develop an MR-compatible sensory stimulation device capable of providing brush stimulation to several positions with separate modules, and to confirm the feasibility of the device by a basic operation experiment and an fMRI experiment. The developed device consists of both an MR-compatible stimulator placed inside the MRI room, a tube-rod mechanism and a driver placed outside the MRI room. The tube-rod mechanism is adopted for power transmission from the driver to the stimulator. Also, in order to provide the stimulation to several positions in the limited space, the device consists of the stimulation module and the positioning module that moves the stimulation module. For the basic operation experiment, we measure a variation of the automated and manual brush stimulation period. For the fMRI experiment, the brush stimulation is provided to the middle fingertip and the palm of a subject in a trial using the developed device. As a result, the standard deviations of the automated brush stimulation period is less than 7.0 ms. This result was smaller than that of the manual stimulation period. Also, the brush stimulation to the fingertip and the palm activated the somatosensory areas respectively. In conclusion, we confirmed the feasibility of the developed device through the experiments.**

I. Introduction

Sensory disturbances are caused by lesions of central or peripheral nervous system, and too little sensation, numbness, too much sensation or paresthesias are common symptoms. In order to evaluate the sensory disturbance, a subjective method is performed, in which the patient answers yes or no orally to a stimulation given by a doctor. Therefore the evaluation result is greatly influenced by subjective factors [1]. The objective evaluation method could contribute to more detailed and correct diagnosis.

fMRI(functional magnetic resonance imaging) is used to investigate the response to sensory stimulation objectively [2]-[4]. fMRI can measure brain activity noninvasively and with high spatial resolution. Therefore fMRI is widely used in neurological field. Stimulating human bodies activates the somatosensory area of the cortex. The activation measured by fMRI could become a useful identification tool for evaluating the sensory disturbance objectively.

In previous studies about a brain activity, when a sensory stimulation is provided, the stimulation is provided manually inside of the MRI room [5]-[7]. The manual stimulation causes an examiner dependent spatial and temporal variance. Using an automated sensory stimulation device might solve this problem. However, use of the devices containing metals and magnetic materials is restricted, because the inside of the MRI room is a high magnetic field environment. Therefore, developing a specialized MR-compatible device is essential.

In the traditional method of evaluating sensory disturbance subjectively, a variety of stimulation are provided to several positions for identifying affected areas and nerves. In the examination of light touch sensation and pain sensation, brush stimulation and pin prick stimulation are usually used [8]. Therefore we adopt those stimulations for use inside of the MRI room.

Among MR-compatible sensory stimulation devices that can provide those mechanical stimulations, a brush stimulation device [9] and a pin stimulation device [10] have been reported. These devices provide only one kind of stimulation respectively. Moreover, the brush stimulation device is limited to one position per setup [9]. The pin stimulation device can provide several positions by parallel systems [10], but an increase of stimulus varieties and stimulation positions makes the device big and complicate. The upsizing of the device should be avoided because the inside of the MRI is narrow. In order to provide some kinds of stimulation to several positions, separating stimulation module and positioning module that moves the stimulation module could be useful.

In this study, we focus the brush stimulation as the stimulation module. The purpose is to develop an MR-compatible sensory stimulation device capable of providing brush stimulation to several positions with separate modules for positioning and stimulation, and to confirm the feasibility of the device by a basic operation experiment and an fMRI experiment.

II. MR-compatible Sensory Stimulation Device

A. Concept of the Stimulation Device

Since fMRI uses a high magnetic field, a use of electromagnetic actuators, electrical circuits and computers inside the fMRI room is strictly limited. Therefore it is necessary to develop a stimulation device which is un affected by high magnetic field.

In this study, the concept of the MR-compatible sensory stimulation device is to consist of three parts, a stimulator inside the MRI room, a tube-rod mechanism and a driver outside the MRI room. An overview of the sensory stimulation device is shown in Fig.1. The stimulator and the tube-rod mechanism are composed entirely of non-magnetic and non-metallic materials. The driver includes actuators and control circuits. The tube-rod mechanism is adopted for the power transmission from the driver to the stimulator. The tube-rod mechanism is composed of a tube and a flexible rod [11]. By pushing and pulling the rod through the tube, mechanical power is transmitted. Therefore, by using the MR-compatible stimulator and the tube-rod mechanism, the sensory stimulation device is available structurally inside the MRI room.

B. System Design of the Stimulation Device

The system configuration of the developed prototype sensory stimulation device is shown in Fig. 2. This device is composed of two modules, a brush stimulation module and a positioning module. Actuators (a linear actuator and a stepping motor) of the driver are controlled by a microcomputer in a control circuit. The parameters for controlling the driver are sent from the PC to the microcomputer by using serial communication. The driver receives the MRI scan signal. Therefore the device can start and stop the stimulation automatically in synchronization with the MRI.

C. Brush Stimulation Module

The configuration of the brush stimulation module is shown in Fig. 3. A linear actuator drives the tube-rod mechanism that transmits a mechanical power from the driver to the stimulator. By reciprocating the linear actuator, the rod in the tube is pushed and pulled; it drives a pinion mechanism, and provides brush stimulation to the human skin. The tube-rod mechanism consists of PTFE tube and acrylic rod. The length of the tube-rod mechanism is about 6m, considering the MRI room we use.

D. Positioning Module

The configuration of the positioning module is shown in Fig. 4. The stimulation unit is moved by using two tube-rod mechanisms. The stimulation part of the brush stimulation module is attached to a stimulation unit of the positioning module. The stimulation position is changed by moving the stimulation unit. A stepping motor and a timing belt drive the two tube-rod mechanisms in parallel. A rod is pushed and the other is pulled synchronously. In order to detect the position of the stimulation unit, a two channels optical linear encoder is equipped in the stimulator. The linear encoder is composed of a slit, red LEDs, phototransistors and optical fibers. Because both the slit and the optical fibers used inside MRI room are made of non-magnetic and non-metallic materials, this encoder system is MR-compatible. By using the encoder signal, the feedback control of the stimulation unit is possible with 1mm resolution.

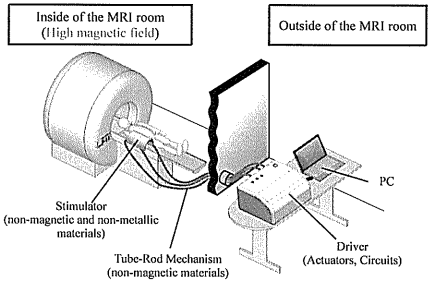

Figure 1. Overview of the sensory stimulation device composed of an MR-compatible stimulator, a tube-rod mechanism and a driver. The stimulator is placed inside the MRI room and the driver is placed outside the MRI room. The tube-rod mechanism is adopted for the power transmission from the driver to the stimulator.

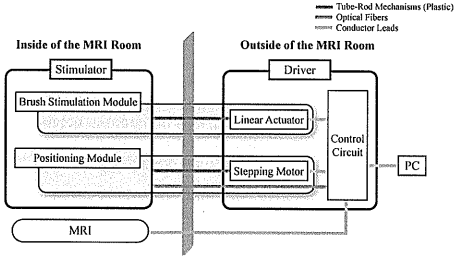

Figure 2. System configuration of the sensory stimulation device. The driver is controlled by PC. The driver receives the MRI scan signal. Since MRI uses a high magnetic filed, components using magnetic and metallic materials: a motor, a linear actuator, and a control circuit are included in the driver. The device is composed of two modules, a brush stimulation module and a positioning module.

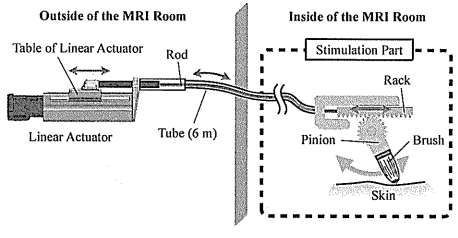

Figure 3. Configuration of the pin stimulation module. By reciprocating the table of the linear actuator, the stimulation head is pushed to human skin and pulled through the rod in the tube repeatedly.

K. Murata is with Cybernics Laboratory, Systems and Information Engineering, University of Tsukuba, Ibaraki 3058573 JAPAN (corresponding author to provide phone and fax: +81-29-853-2883; e-mail: murata at golem.kz.tsukuba.ac.jp).

A. Matsushita, K. Saotome and H. Kawamoto are with Center for Cybernics Research, University of Tsukuba, Tsukuba, Ibaraki 3058573 JAPAN (e-mail: akira at ccr.tsukuba.ac.jp, saotome at ccr.tsukuba.ac.jp, kawamoto at golem.kz.tsukuba.ac.jp).

Y. Sankai is with Cybernics Laboratory, Faculty of Engineering, Information and Systems, University of Tsukuba, Ibaraki 3058573 JAPAN (e-mail: sankai at golem.kz.tsukuba.ac.jp).

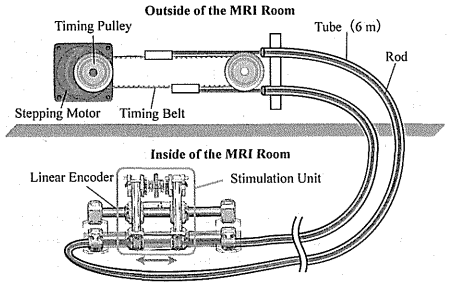

Figure 4. Configuration of the positioning module. The stepping motor drives 2 rods in the tubes at a time, and the stimulation unit is driven linearly. The position of the stimulation unit is detected by the linear encoder.

III. Experiment

In this study, we perform a basic operation experiment and an fMRI experiment for confirming the feasibility of the developed device.

A. Basic Operation Experiment

A basic operation experiment is performed to evaluate the performance of the brush stimulation module of the developed device.

In this device, the brush stimulation is provided by reciprocating the brush. The variable parameter of this brush stimulation is the frequency. Therefore we examine the modulation performance of the frequency of the brush stimulation. Moreover, to examine the stability of the automated brush stimulation, we measure and compare a variation of the automated brush stimulation frequency of the developed device and a variation of the manual brush stimulation frequency. This experiment is conducted in the laboratory environment that separated the stimulator and the driver 6m. This 6m distance is the same as the condition in which the MRI experiment is conducted. To measure the frequency of the brush stimulation, in the case of the automated stimulation using the device, an experimental system shown in Fig. 5 (a) is used. And, in case of the manual stimulation, an experimental system shown in Fig. 5 (b) is used. A douser is attached in the stimulation head instead of a brush. A photo interrupter (CNZ1023, Panasonic) detects a moment that the douser passes through, and the period of the brush stimulation is calculated. In the case of automated stimulation, the input frequency is adjusted from 1Hz to 5Hz in steps 1Hz. In the case of manual stimulation, participants are given the reference of the frequency (1Hz, 3Hz and 5Hz) using a metronome. Three times of a 30 seconds measurement are performed, and an average and a standard deviation of the period are calculated. Experiment participants who perform manual brush stimulation are 5 participants.

B. fMRI Experiment

In fMRI experiment, we verify that the brush stimulation of the developed device activates somatosensory areas.

Since the part used inside MRI room of the developed device is composed of non-magnetic and non-metallic materials, the device does not affect MR images and is not affected by high magnetic field of MRI. Therefore the safety of the device for MRI is secured structurally. In this experiment, the providing stimulation is 2Hz brush stimulation to right middle fingertip and right palm of a healthy subject alternately as shown in Fig. 6. A diagram of a task sequence is shown Fig. 7. A task consists of 30 seconds stimulation to a middle fingertip following 30 seconds rest then 30 seconds stimulation to a palm following 30 seconds rest. At the each rest, stimulation unit is moved from the palm to the fingertip or from the fingertip to the palm. The task is repeated 4 times in a trial.

In this experiment, the head of the subject is fixed by using sponges and headphone attached to the MRI. The subject lies supine and equipped the stimulator with right hand. Putting cushions under the right arm, the subject had relaxed posture. The environment of the experiment is shown in Fig. 8. And the subject's hand equipped with the developed stimulator is shown in Fig. 9. The fMRI experiment is performed in University of Tsukuba, on a 3.0T MRI (Achieva 3.0T TX Release 3.2.1.1, PHILIPS) equipped with a 32 channel SENSE head coil. In order to secure the enough safety of the subject, this experiment is performed with a radiological technologist and a medical doctor.

MR images obtained by the fMRI experiment are analyzed using SPM8 (Welcome Department of Cognitive Neurology, http://www.fil.ion.ucl.ac.uk/spm) on MATLAB (Math Works). Functional images are normalized into standard stereotactic space using the Montreal Neurological Institute template (MNI) [12]. A stringent statistical threshold with family-wise error correction $p < 0.05$ has been applied.

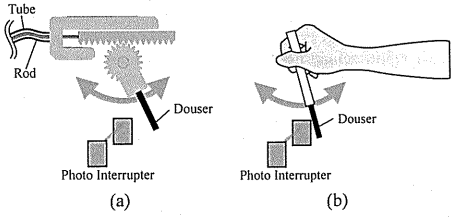

Figure 5. Diagram of the experimental system for measuring the period. The photo interrupter detects a moment that the douser passes through. (a) is the system in case of the automated stimultion by the developed device, and (b) is the system in case of the manual stimulation by the participants.

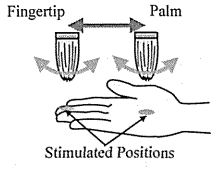

Figure 6. Diagram of the stimulation positions of the fMRI experiment. The brush stimulation is provided to the middle fingertip and the palm.

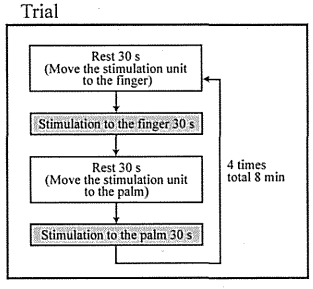

Figure 7. Diagram of the task sequence of the fMRI experiment. A task consists of 30 seconds stimulation to a middle fingertip following 30 seconds rest then 30 seconds stimulation to a palm following 30 seconds rest. At the each rest, stimulation unit is moved from the palm to the fingertip or from the fingertip to the palm. The task is repeated 4 times in a trial.

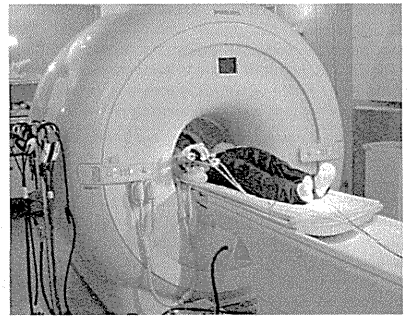

Figure 8. Environment of the fMRI experiment. Stimulation is peovided to right hand of a healthy subject by using developed sensory stimulation device in the MRI room.

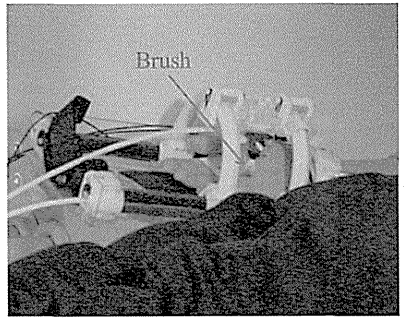

Figure 9. Subject's hand equipped with the developed stimulator. The brush stimulation is provicded to the palm in the MRI.

IV. Result

A. Basic Operation Experiment

A result of the basic operation experiment is shown Fig.10. Fig.10 (a) shows the relationship between the input frequency and the output frequency from 1 Hz to 5 Hz. The input frequency is the frequency of the linear actuator movement, and the output frequency is the frequency of the stimulation head movement. A correlation coefficient between the input frequency and the output frequency is 0.999. Therefore the frequency of the brush stimulation module can be linearly controlled between 1 Hz and 5 Hz.

Fig. 10 (b) shows the relationship between the average and the standard deviation of the period of the manual and automated stimulation of 1 Hz, 3 Hz and 5 Hz. The standard deviation of the manual stimulation period is more than 19.3 ms and the standard deviation of the automated stimulation period is less than 7.0 ms. Therefore the standard deviation of the automated stimulation period is less than that of the manual stimulation period. Moreover, in the case of the manual stimulation, the standard deviation of the period increases as the average of the period increases compared with the automated stimulation.

B. fMRI Experiment

Brain responses of a subject according to the brush stimulation to the right middle fingertip and the right palm are shown in Fig. 11 (a) and Fig. 11 (b). Activation of the left somatosensory area was observed respectively.

V. Discussion

In the basic operation experiment, we examined the modulation and stability of the brush stimulation frequency in the environment that separated the stimulator and the driver 6 m. The correlation coefficient between the input frequency and the output frequency was 0.999. Therefore we verified that the frequency of the brush stimulation module could be linearly controlled between 1 Hz and 5 Hz. Moreover, the standard deviation of the automated stimulation period was less than that of the manual stimulation period, and we

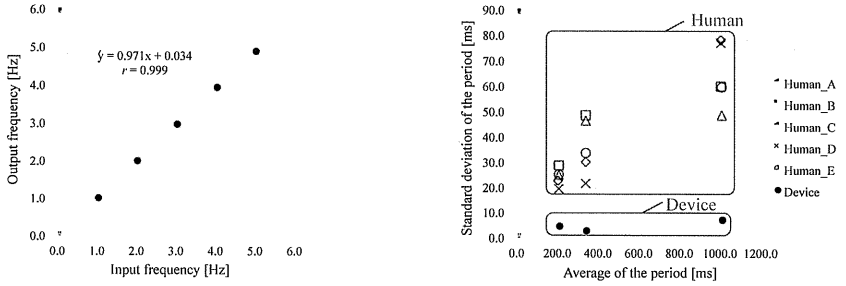

(a) (b)

Figure 10. Result of the frequency control experiment of the brush stimulation (a) The relationship between the input frequency and the output frequency of the brush stimulation by the developed device. (b) The relationship between the average of the period and the standard deviation of the period in the brush stimulation by human and the developed device.

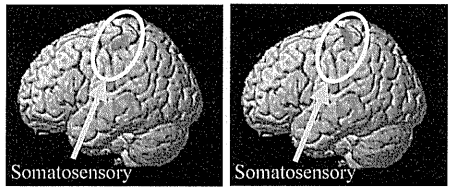

(a) (b)

Figure 11. Brain responses of a subject according to the brush stimulation to the right middle fingertip (a) and to the right hand (b). (Family- wise error corrected p<0.05) Activation of left somatosensory area was observed respectivel.

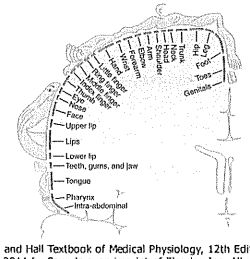

Figure 12. Representation of the difference areas of the body in somatosensory area [13].

verified that the developed device could provide the brush stimulation with stable frequency. Thus, whoever performs the examination, the stable stimulation is available by using the developed device. This stability is very important for developing the objective method of the sensory disturbance with many subjects in the future.

In the fMRI experiment, the brush stimulation was provided to the middle fingertip and the palm of a subject in a trial using the developed device. As a result, the stimulation of the developed device can activate the somatosensory area in the both cases. Furthermore, positional relationship between the activated area of the stimulating fingertip and palm (Fig. 11) is similar to Fig. 12. Fig. 12 shows a somatotopic organization schematized correspondence of somatosensory and each part of human body. Therefore the developed device was able to stimulate the several positions and we observed the possibility of the somatotopic organization. Thus, providing the brush stimulation and moving stimulation position can be realized inside the MRI room in a trial using the developed device. Those function could contribute to identifying affected areas of sensory disturbance.

In this study, the device is separated the stimulation module and the positioning module. The positioning module moves the stimulation module, and the device provides the stimulation to several positions. This configuration would avoid the upsizing and the complication of the device. Moreover, the change of stimulus varieties is easy using this configuration. It is assumed that this configuration is useful for providing a variety of the stimulation to the various positions.

VI. Conclusion

In this study, we developed a novel MR-compatible sensory stimulation device capable of providing brush stimulation to several positions with separate modules for positioning and stimulation, and confirmed the feasibility of the device by a basic operation experiment and an fMRI experiment. In the basic operation experiment, we verified that the frequency of the brush stimulation module could be linearly controlled between 1 Hz and 5 Hz and that the developed device provided brush stimulation of less frequency variation as compared with that of the manual stimulation. In the fMRI experiment, we verified that the brush stimulation to the fingertip and the palm using the developed device activated the somatosensory areas respectively.

In our future work, we intend to develop other varieties of stimulation module, for example pin prick and vibration stimulation. Furthermore, we apply this device to various subjects and examine the relationship the stimulation of the device and brain response for developing the objective method of the sensory disturbance.

Acknowledgment

This study was supported by the "Center for Cybernics Research (CCR) - World Leading Human-Assistive Technology Supporting a Long-Lived and Healthy Society" granted the "Funding Program for World-Leading Innovative R&D on Science and Technology (FIRST Program)," initiated by the Council for Science and Technology Policy (CSTP).

References

[1] W. W. Campbell, *DeJong's The Neurologic Examination seventh edition*, Philadelphia: Lippincott Williams & Wilkins, 2012, p. 518.
[2] E. Disbrow, M. Buonocore, J. Antognini, E. Carstens and H.A. Rowley, "Somatosensory cortex: a comparison of the response to noxious thermal, mechanical, and electrical stimuli using functional magnetic resonance imaging," Human Brain Mapping, vol. 6, no. 3, 1998, pp. 150-159.
[3] S. Petra, G. Chris, B. Jonathan, M. Henry, J. Tim, C. Iain, B. Chas and T. Irene, "An fMRI study of cerebral processing of brush-evoked allodynia in neuropathic pain patients," NeuroImage, vol. 32, no. 1, 2006, pp. 256-265.
[4] C. L. Reed, R. L. Klatsky and E. Hlgren, "What vs. where in touch: an fMRI study", NeuroImage, vol. 25, no. 3, 2005, pp. 718-726.
[5] F. Z. Yetkin, W. M. Mueller, T. A. Hammeke, G. L. 3rd Morris and V. M. Haughton, "Functional magnetic resonance imaging mapping of the sensorimotor cortex with tactile stimulation," Neurosurgery, vol. 36, no. 5, 1995, pp. 921-925.
[6] I. M. Christopher, E. S. Chantal, C. Suzanne, F. Bruce, C. G. Annette, R. R. Bruce and M. D. Anders, "Segregation of somatosensory activation in the human rolandic cortex using fMRI," Neurophysiology, vol. 84, no. 1, 2000, pp. 558-69.
[7] G. D. Iannetti, C. A. Porro, P. Pantano, P. L. Romanelli, F. Galeotti and G. Cruccu, "Representation of different trigeminal divisions within the primary and secondary human somatosensory cortex," Neuroimage, vol. 19, no. 3, 2003, pp. 906-912.
[8] V. W. Lin, C. M. Bono, D. D. Cardenas, N. C. Cutter, F. S. Frost, M. C. Hammond, L. B. Lindblom, I. Perkash, R. Waters and R. M. Woolsey, *Spinal Cord Medicine Principles and Practice*, New York: Demos Medical Publishing, 2003, ch 27.
[9] S. J. Graham, W. R. Staines, A. Nelson, D. B. Plewes and W. E. McIlroy, "New devices to deliver somatosensory stimuli during functional MRI," Magnetic Resonance in Medicine, vol. 46, no. 3, 2001, pp. 436-442.
[10] C. Dresel, A. Parzinge, C. Rimpau, C. Zimmer, A. O. Ceballos-Baumann and B. Haslinger, "A new device for tactile stimulation during fMRI," NeuroImage, vol. 39, no. 3, 2008, pp. 1094-1103.
[11] K. Kishi, M. Fujie, M. Hashizume, I. Sakuma and T. Dohi, "MR-compatible Surgical Support Manipulator System with Rod-driven Instruments," Journal of Robotics Society of Japan, vol. 27, no. 6, 2009, pp. 652-660 (in Japanese).
[12] K. J. Friston, J. Ashburner, C. D. Frith, J.-B. Poline, J. D. Heather and R. S. J. Frackowiak, "Spatial registration and normalization of images." Human Brain Mapping, vol. 3, vol.3, 1995, pp. 165-189.
[13] E.H.John, *Textbook of medical physiology 12th ed*, Philadelphia: Saunders, 2011, p. 576.

技術論文

装着型歩行補助ロボットのリスク管理方法
ロボットスーツ HAL® 福祉用の事例

鍋嶌厚太[*1] 新宮正弘[*1] 河本浩明[*2] 山海嘉之[*2*3]

Risk Management for Wearable Walking Assistant Robot
A Case Study of Robot Suit HAL® for Well-being

Cota Nabeshima[*1], Masahiro Shingu[*1], Hiroaki Kawamoto[*2] *and* Yoshiyuki Sankai[*2*3]

In this paper, we provide a essence of the risk management sheet that was used to obtain the world-first certificate of ISO/DIS 13482:2011 for "Robot Suit HAL® for Well-being," and discuss how it could be applicable to more common wearable walking assistant robots. We hope our experiences and knowledge will help overcoming the so-called "valley of death" towards commercialization of the personal care robots.

Key Words: Robot Suit HAL®, Physical assistant robot, Risk management, Quality management, International safety standards

1. はじめに

CYBERDYNE 株式会社 (以下, CD 社) は, 筑波大学のサイバニクス研究から生まれた装着型ロボット "ロボットスーツ HAL®" [1] (以下, HAL) を実用化し, 広く社会に貢献すべく 2004 年に設立された. 2008 年には, CD 社初の製品となる "ロボットスーツ HAL® 福祉用" [2] (以下, HAL 福祉用) のレンタル・リース販売を開始した.

CD 社はその当初より, 安全を最優先に HAL の研究開発, 製造, 販売に取り組んできた. しかし当時は装着型ロボットの安全標準が確立されておらず, HAL 福祉用の安全性について, 第三者評価, すなわち, 認証を受けられずにいた. そのため安全標準への適合という簡便な安全性の証明を利用できず, CD 社は, 顧客に都度, HAL 福祉用の安全性について説明する必要があった.

安全標準への適合をもって安全性の証明を簡便に行うことは, メーカーだけでなく, 消費者, 規制当局にも便益をもたらし, 産業化を促進すると考えられる. そのため CD 社は筑波大学とともに, HAL 福祉用を主なプラットフォームとして, 新エネルギー・産業技術総合開発機構 (NEDO) が 2009 年〜2014 年の期間で実施する生活支援ロボット実用化プロジェクト [3] に参画し, 装着型ロボットの安全技術と安全性検証手法の研究開発を行い, また, その成果を国際標準化すべく活動してきた.

2011 年には, これらの活動の成果として, 国際安全規格原案 ISO/DIS 13482:2011 "Robots and robotic devices - Safety requirements for non-industrial robots - Non-medical personal care robot" [4] が, ISO/TC184/SC2/WG7 により発行, 公開された[†]. これにより初めて, HAL 福祉用の安全性について第三者評価が可能となった. CD 社は現行モデルの HAL 福祉用に対する ISO/DIS 13482:2011 認証を, 一般財団法人 日本品質保証機構 (JQA) に依頼し, 2013 年 2 月に, ISO/DIS 13482:2011 の世界初の認証を得ることができた [5].

ISO/DIS 13482:2011 では, [6]〜[9] などの国際安全規格と同様に, リスクアセスメントが要求されている [10]. そのためメーカーが認証を取得する際には, 対象となる機器のリスク管理表を認証機関に提出する必要がある. 本論文では, Sec.2 で HAL 福祉用の特徴を述べたのち, Sec.3 で, 実際に認証機関に提出した HAL 福祉用のリスク管理表の一部を示し, CD 社がどのようにリスク管理を実施したかを述べる. HAL 福祉用のリスク管理表の構成は, 一般的な装着型歩行補助ロボットに対しても, 標準的に適用できると考えられる (Sec.4). 本論文が, 装着型歩行補助ロボットのみならず, 装着型ロボット, ひいては, 生活支援ロボットの実用化および産業化の一助となることを期待する.

原稿受付
[*1]CYBERDYNE 株式会社
[*2]筑波大学システム情報系
[*3]筑波大学サイバニクス研究センター
[*1]CYBERDYNE Inc.
[*2]Faculty of Engineering, Information and Systems, University of Tsukuba
[*3]Center for Cybernics Research, University of Tsukuba

[†]ISO 規格は, その策定の段階に従って, 委員会原案 (CD), 国際規格原案 (DIS), 最終国際規格原案 (FDIS), 国際規格 (IS) と発行される. DIS 以降は一般に入手可能となり, 認証が可能となる. ただし, FDIS 発行後は DIS が入手できなくなるため, DIS での認証は行われなくなる. ある製品が DIS で認証を取得していた場合, IS 発行後には必要に応じて, 改めて IS による認証を取得することになる. 一般的には DIS 以降, 要求が大きく変わることは少ないため, DIS 認証を取得した製品の IS に対する適合性評価は, 差分的に行われる.

Fig. 1 The Robot Suit HAL® for Well-being.

2. HAL 福祉用の特徴

HAL 福祉用は, 装着者の下肢運動の支援を意図した外骨格型の装着型ロボットであり, 歩行や立ち座りの際の主要な関節 (股関節と膝関節) に沿う形で能動軸を有している. 装着の様子および外観を Fig.1 に, 構造の模式図を Fig.2 に示す. HAL 福祉用のフレームは足裏で床面に接地しており, HAL 福祉用の重量が装着者の負荷にならないと同時に, 装着者の体重がフレームの負荷にならない構造となっている.

詳細には立ち入らないが, HAL 福祉用では, 装着者の膝と大腿に貼り付けられた電極から読み取った生体電気信号を利用し, 装着者の筋肉が動くより早くモーターを駆動することでアシストを行う "サイバニック随意制御" と, 装着者の関節角度, 姿勢, 体重移動の情報から推定した歩行フェーズに基づくアシストを行う "サイバニック自律制御" を混合した制御方式が用いられている.

以上の特徴から, その意図する使用において, HAL 福祉用と装着者は電気的に接続されるだけでなく, 互いに接触し, 力学的エネルギーをやりとりする. つまり本質的に, 機械的, 電気的, 熱的, 音響的なハザード源となる機器を装着者から隔離できない. これは産業用ロボットで一般的な "隔離の原則" を単純には適用できないことを意味し, 特に装着型ロボットにおいては, その安全性が懸念される原因となっている. HAL 福祉用では, Sec.3 のようにリスク管理を実施し, 個別のハザードごとに十分なリスク低減を講じることで, 安全性を確保している.

3. HAL 福祉用のリスク管理

HAL 福祉用は 2013 年 9 月末の時点で, 国内 160 施設, 400 台以上が稼働しており, 累積の利用者は 4,000 人以上[†]に上っている. HAL 福祉用において, これまでに有害事象は発生しておらず, 安全面での実績を有していると言える. このことは, 以下で示す HAL 福祉用に適用されたリスク管理の有効性を示していると考えられる.

[†]CD 社による, 稼働ログに基づく推計.

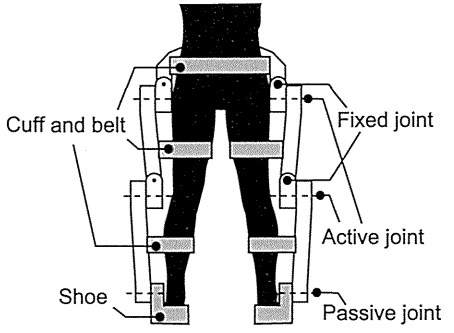

Fig. 2 The abstract structure of Robot Suit HAL® for Well-being.

3.1 CD 社のリスク管理体制

製品の安全は品質の一部 [7] であり, 製品のライフサイクルのすべて (初期の構想, 設計開発, 仕入れ, 製造, 引き渡し, 保守サービス, 苦情, 回収・廃棄など) に係わる. CD 社では, リスク管理システムが組み込まれた一般的な品質管理システムを有しており, 組織的にリスク管理プロセスに取り組んでいる. その結果として, CD 社は 2012 年 12 月に, 医療機器の品質マネジメントシステムの国際規格である ISO 13485:2003 の認証を, 株式会社 UL Japan より取得している [11].

3.2 HAL 福祉用のリスク管理表

HAL 福祉用のリスク管理には表を用いた (リスク管理表). これは特定したハザード, 推定した初期リスク, 特定したリスク低減方法, 期待されるリスク低減後のリスクについて一覧性を持たせるためである. ハザードの特定, 初期リスクの推定, リスク低減方法の特定は, ISO 14971:2007 [7] をベースに, HAL 福祉用の開発, 製造, 販売および市場からのフィードバックにより得られた知見を利用して行った.

初期リスクの推定にあたって, 当初は加算法を用いていたが, 現在ではよりリスク低減方法の効果を表現しやすいマトリクス法を用いた [12]. リスク管理にあたって定義したリスクマトリクスを Table 1, Table 2 に示す. なお, 通常のマトリクス法では, 危害の重大さと危害の頻度のマトリクス (Table 2) のみを用いるが, 危害に至る事象の発生と遷移を表現できなかったため, Table 1 を追加した.

Table 1, Table 2 では, 加算法や積算法を用いずにレベルを割り当てている. これは,

- 一度死亡に至る危害が特定された場合, リスク低減をいくら講じても, リスクを受容可能にできない
- 算出されたリスクの値が, 必ずしもリスク低減の優先度に一致しない
- 発生頻度や遷移可能性に割り当てた数値自体に任意性があり, 加算あるいは積算によって求められる数値に対して, 実質的な意味付けが難しい

といった, 数値化に起因する問題を避けるためである. また, リスクグラフは, 加算法や積算法同様, リスクの値にリスク低減の

優先度を反映しにくく，さらに，事象の遷移を表現すると複雑化することから，不採用とした．実際の製品開発では，ALARP 原則に従って網羅的にリスク低減を講じるため，その指針となる，直感に合ったレベル付けができれば十分と言える．そのため，HAL 福祉用では，Table 1，Table 2 から構成されるマトリクス法を採用した．

Table 1 は，発生頻度 Fx の { ハザード，危険状態 } が発生した結果として，遷移可能性 Tx で別の { ハザード，危険状態，危害 } が発生するときの発生頻度 Fx' を割り当てるマトリクスである．Table 2 は，発生頻度 Fx で危害が発生するとして，その危害の重大さが Sx のときのリスクレベルを，I から IV の 4 段階で割り当てるマトリクスである．HAL 福祉用では，リスクレベルが I なら受容可能なリスク，II なら受容可能だが追加のリスク低減を検討するリスク，III，IV なら受容できないリスクとした．

HAL 福祉用のリスク管理表は，危険状態表とハザード表の 2 表構成とした．HAL 福祉用に関するリスクの構造として，危害に至る事象の遷移 (ハザード ⇒ 危険状態 ⇒ 危害) を想定した場合，

- 危害は，必ず危険状態，すなわち “有害なエネルギーが人体にさらされる状況” を経て発生する
- 危険状態の種類はそれほど多くないが，危険状態に遷移するハザードの種類は多い

という特徴がある．リスク管理表を 2 表構成とすることで，リスクの構造を活かし，見通しの良いリスク管理表を作成できると考えられた．なお，ISO/DIS 13482:2011 の認証取得に用いたリスク管理表には，危険状態 16 種，および，ハザード 170 種が含まれていた．

HAL 福祉用のリスク管理を進めていく上で，2 表構成のリスク管理表には，以下の利点があった:

Table 1 Occurrence frequency and its transfer possibility of {hazard, hazardous situation, harm}

		Transfer possibility			
		T1	T2	T3	T4
Occurrence frequency	F1	F1'	F1'	F2'	F2'
	F2	F1'	F2'	F2'	F3'
	F3	F2'	F2'	F3'	F3'
	F4	F2'	F3'	F3'	F4'

Fx, Fx' are the occurrence frequencies of {hazard, hazardous situation, harm} as,
x=1: “never,”
x=2: “rare,”
x=3: “occasional,”
x=4: “often.”

Tx is the transfer possibility (avoidability) from {hazard, hazardous situation} to {hazard, hazardous situation, harm} as,
x=1: “never” (“easy to avoid”),
x=2: “rare” (“possible to avoid”),
x=3: “occasional” (“difficult”),
x=4: “often” (“impossible”).

[利点 1] ある一つのリスク低減方法が，

- ハザードが起こるのを防ぐ
- ハザードが危険状態に遷移するのを防ぐ
- 危険状態が起こるのを防ぐ
- 危険状態が危害に遷移するのを防ぐ
- 危害の重大さを下げる

のいずれの効果を持つかを検討しやすい．

[利点 2] 危害に至る事象の遷移において，

- 故障や誤使用など，異なるハザードが 1 つの危険状態に遷移する場合，
- 故障検出などが機能して，ハザードが危険状態に遷移しない場合，
- 危険状態が生じても，人が容易に回避できる場合，
- 危険状態でも人に印加されるエネルギーが低い場合

などを表現しやすい．

[利点 3] 安全規格で言及されている危険状態，ハザード，リスク低減方法の対応関係を表現しやすい．

HAL 福祉用のリスク管理表全体では，危害をトップノードとしたツリー構造を成したため，FTA のようなトップダウンの性質を有し，また一方では，ソフトウェアと電気系に対してシステムレベルの FMEA を行い，故障や機能失敗のハザードをハザード表に列挙したため，ボトムアップの性質も同時に有することになった．

具体例として，感電リスクがどのようにリスク管理表で管理されるかを，Table 3 (危険状態表)，Table 4 (ハザード表) に示す．感電リスクは，HAL 福祉用と装着者が電気的に接続されているために，その評価と低減を適切に実施すべきリスクである (Sec.2 参照†)．

Table 3 の 2 行目は，危険状態 A “装着者が触れる部位に電位差が現れる/漏れ電流が流れる” について，初期リスクの評価を行っている．該当部位に装着者が気付かずに触ることで，感電による火傷が生じると想定している．初期リスクのリスクレベルは III であり，受容できないリスクとなっている．このリスクを

Table 2 Definition of risk level

		Severity of harm			
		S1	S2	S3	S4
Occurrence frequency of harm	F1	I	I	I	II
	F2	I	I	II	III
	F3	I	II	III	IV
	F4	II	III	IV	IV

I, II, III, IV are the risk levels.

Sx is the severity of harm as,
x=1: “no injury,”
x=2: “curable or minor injury”
e.g. cut or scrape of skin,
x=3: “incurable or serious injury”
e.g. loss of fingers or limbs,
x=4: “mortal injury.”

†機械的な接触によるリスクの評価と低減は，[13] [14] を参照．

低減できたかは，最終的に漏れ電流試験を行うことで確認するとしている．

Table 3 の 3 行目では，リスク低減方法として安全電圧を採用し，危害の重大さを軽度 (S2) にできると見積もっている．このとき，危険状態の発生頻度が高くとも，リスクレベルが II となり，受容可能となる．このリスク低減方法の実施は，電源仕様の検査によって確認するとしている．なお，安全電圧の採用は，機械安全における 3 ステップメソッドの本質的安全設計方策にあたり，優先的に検討すべきリスク低減方法である．

危険状態 A の発生頻度を低くし，よりリスクを下げるには，原因となるハザードから遷移する可能性を下げれば良い．Table 3 の 4 行目の受容可否の欄の “OK+” は，リスク低減が追加して行われることを示している．

危険状態 A に遷移するハザードとして，Table 4 の 2 行目と 4 行目それぞれに，ハザードを例示している．ハザード 1 は，電源線が外れて外装に触れるハザードであり，ハザード 2 は，外装の割れから電源線が露出するハザードである．これらのハザードの発生頻度は，関係する部位の強度を高めることで下がると期待できる．それぞれに対するリスク低減方法は，3 行目と 5 行目に記されている．これらのリスク低減方法の実施は，強度計算や，強度試験によって確認できるとしている．なお，これらのリスク低減方法は，機械安全における 3 ステップメソッドの安全防護・付加保護方策にあたる．

Table 4 の 6 行目には，典型的な誤使用として，使用者が機器に水をこぼすハザードが示されている．HAL 福祉用の使用環境は屋内のトレーニング施設であり，また，電子機器に水を掛けないことは一般的となっているため，発生頻度はまれに起こる (F2) としている．7 行目には，水が掛かることで生じる短絡を検出し，電流を遮断するとしている．これは機械安全における 3 ステップメソッドの安全防護・付加保護方策であり，危険状態 A への遷移可能性を T4 から T3 に下げられるとしている．なお，短絡検出による電流遮断は，感電のリスク低減だけでなく，火災のリスク低減にも有効であり，実際のリスク管理表では複数回登場している．

Table 4 の 8 行目には，機器に水をこぼす誤使用のハザードを防ぐために，注意を行うとしている．注意は一般的に取扱説明書に記載されるため，リスク低減方法の実施は取扱説明書の記載によって確認できるとしている．なお，このようなリスク低減は，機械安全における 3 ステップメソッドの使用上の情報にあたる．

Table 4 では，列挙されたハザードが直接危害につながらないため，危害の重大さとリスクレベルの割り当てを行っていない．またこの例では，Table 3 を利用することで，“危険状態 A につながるハザードはすべて受容可能である” ところから初められるため，ハザード表ではリスクレベルの割り当てに悩むこと無く，ハザードを列挙し，追加のリスク低減を講じて行くことができる．

Table 3, Table 4 では，検証に用いる試験の例として，漏れ電流試験，電源線の引張試験，外装の強度試験が挙げられている．これらの試験を実際に行う場合には，適切な安全規格 ([9] など) で定められている試験方法と合格基準を利用できる．

3.3 リスク低減方法の検証と妥当性確認

HAL 福祉用では，リスク管理表に記載したリスク低減方法のすべてについて CD 社で検証を実施した．特に受容できないリスクを受容可能なレベルまで下げているリスク低減方法については，重点的に安全性試験を行うようにした [13] [14]．ISO/DIS 13482:2011 の認証を受ける際は，認証機関が第三者として，規格の要求に対する適合性を評価すべく，検証を行った．

具体的な検証方法としては，レビュー，検査，試験の他に，安全規格に定められた安全性評価法を採用した．例えば生物学的安全性や EMC，材料，バッテリーなど個別の安全規格が存在する場合には，規格適合を検証方法として採用した (Sec.3. 2 参照)．

HAL 福祉用では，最終的なリスク低減方法となる情報提供を，取扱説明書の記載と表示における禁止，警告，注意によって行った．禁止，警告，注意の別は，その情報によって低減されるリスクの程度をリスク管理表から特定し，決定した．情報提供に関する検証はチェックリストを用いて行い，必要な情報の記載に漏れが無いかを確認した．

全体的なリスク管理の妥当性を確認するために，リスク管理表に記載したリスク低減方法を個別に検証したのちに，実際のユースケースを模擬した試験を実施した．この妥当性確認において，新たなハザードが生じないことを確認した．

4. おわりに

本論文は，NEDO が実施する生活支援ロボット実用化プロジェクトの成果の一部として，CD 社が HAL 福祉用に対して実施したリスク管理の方法を，リスク管理表を中心に述べた．このリスク管理の方法はあくまで現状を示したものであり，今後の改善の結果として変更される可能性がある．例えばリスク管理を表からデータベースに移したり，情報システムを利用して市場からのフィードバックを得やすくすることで，リスク管理にかかる労力を低減できると考えられる．

本論文では，HAL 福祉用のリスク管理に適用した，2 表構成のリスク管理表を示した．この方法は，危険状態の種類が把握可能な程度に収められ，かつ，ハザードが瞬時に危害に発展しない場合に有効と考えられる (Sec.3. 2 参照)．人が危害を受ける対象であれば，“有害なエネルギーが人体にさらされる” 危険状態の種類は，{ 機械的，熱的，電気的，化学的 } エネルギーの授受など，あまり多くないと言えるため，本論文のリスク管理方法を適用しやすいと思われる．そのため，本論文のリスク管理方法は，主に使用者/装着者が危害を受けることになる生活支援ロボット，特に装着型ロボットのリスク管理に有効と考えられる．本論文が，装着型ロボットのみならず，生活支援ロボットの実用化および産業化に必須となるリスク管理において，有益な情報となることを期待する．

謝辞 本研究は，独立行政法人新エネルギー・産業技術総合開発機構 (NEDO) の委託業務および，内閣府最先端研究開発支援プログラム「健康長寿社会を支える最先端人支援技術研究プログラム」の支援により行われた．

参考文献

[1] H. Kawamoto and Y. Sankai. Power assist system HAL-3 for gait disorder person. In *Proceedings of the 8th International Conference on Computers Helping People with Special Needs*, pp. 196–203, London, UK, 2002.

Table 3 A part of the risk management sheet for hazardous situation against electrical shock

ID	Hazardous situation	Possible harm	Risk control measure	F	T	F'	S	R	Acceptability	Verification method
A	Potential difference / leakage current between touchable parts	electrical burn injury	-	F4	T3	F3'	S3	Ⅲ	NG	Leakage current test
-	-	-	Application of safety voltage	F4	T3	F3'	S2	Ⅱ	OK	Inspection of specification of the power supply
-	-	-	Reduction of transfer possibility from hazards resulting in the hazardous situation A	F2	T3	F2'	S2	I	OK+	Inspection of the risk management sheet for hazards

Table 4 A part of the risk management sheet for hazard against electrical shock

ID	Hazard	Possible hazardous situation	Risk control measure	F	T	F'	Verification method
1	Power wire that came off touches to the enclosure.	Hazardous situation A	-	F4	T4	F4'	-
—	-	-	Application of double fixation	F1	T4	F2'	Inspection of assembling manual / tensile test
2	Power wire exposures through the broken enclosure.	Hazardous situation A	-	F4	T4	F4'	-
—	-	-	Sufficient mechanical strength of enclosure	F1	T4	F2'	Inspection of the strength calculation / strength test
3	A user spills water on the equipment.	Hazardous situation A, electrical short	-	F2	T4	F3'	-
—	-	-	Short circuit detection and current interruption	F2	T3	F2'	Inspection of the drawings / short-circuit test
—	-	-	Precaution by instruction for use	F1	T3	F2'	Inspection of the user manual

[2] CYBERDYNE Inc. Robot Suit HAL for Well-being. http://www.cyberdyne.jp/english/customer/index.html.

[3] 新エネルギー・産業技術総合開発機構 (NEDO). 生活支援ロボット実用化プロジェクト. http://www.nedo.go.jp/activities/EP_00270.html, 2009-2014.

[4] ISO. *ISO/DIS 13482: Robots and robotic devices – Safety requirements for non-industrial robots – Non-medical personal care robot*. International Organization for Standardization, Geneva, Switzerland, 2011.

[5] 一般財団法人 日本品質保証機構 (JQA). 世界初、ISO/DIS 13482 に基づくパーソナルケアロボットの認証 – CYBERDYNE 株式会社へ認証書を発行 –. http://www.jqa.jp/service_list/fs/topics/topics_fs_04.html, 2013.

[6] ISO. *ISO 12100: Safety of machinery – General principles for design – Risk assessment and risk reduction*. International Organization for Standardization, Geneva, Switzerland, 2010.

[7] ISO. *ISO 14971: Medical devices – Application of risk management to medical devices*. International Organization for Standardization, Geneva, Switzerland, 2007.

[8] IEC. *IEC 61508-1 Ed.2.0: Functional safety of electrical/electronic/programmabl electronic safety-related systems – Part 1: General requirements*. International Electrotechnical Commission, Geneva, Switzerland, 2010.

[9] IEC. *IEC 60601-1 Ed.3.0: Medical electrical equipment – Part 1: General requirements for basic safety and essential performance*. International Electrotechnical Commission, Geneva, Switzerland, 2005.

[10] 鍋嶌厚太, 河本浩明, 山海嘉之. 装着型歩行補助ロボットのための ISO 13482 要求分析. ロボティクス・メカトロニクス講演会 2013 (ROBOMEC2013), 茨城, 2013. 1A1-H09.

[11] UL Japan. 医療機器の品質マネジメントシステム – 国際規格、ISO 13485:2003 の認証発行 – 世界初ロボット治療機器「医療用 HAL」の社会実装を目指す CYBERDYNE 株式会社に. *JAPAN ON the MARK*, Vol. 44, p. 4, 2013.

[12] C. Nabeshima, H. Kawamoto, and Y. Sankai. Typical risks and protective measures of wearable walking assistant robots. In *Proceedings of 2011 IEEE/SICE International Symposium on System Integration (SII2011)*, pp. 914–919, Kyoto, Japan, 2011.

[13] C. Nabeshima, H. Kawamoto, and Y. Sankai. Strength testing machines for wearable walking assistant robots based on risk assessment of Robot Suit HAL. In *Proceedings of 2012 IEEE International Conference on Robotics and Automation (ICRA 2012)*, pp. 2743–2748, Minnesota, USA, 2012.

[14] 鍋嶌厚太, 河本浩明, 山海嘉之. 装着型歩行補助ロボットのリスク分析と安全性試験法. 日本ロボット学会誌, Vol. 30, No. 8, pp. 752–758, 2012.

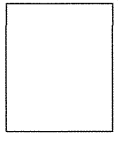

鍋嶌厚太 (Cota Nabeshima)

2009 年東京大学大学院情報理工学系研究科修了. 博士 (情報理工学). 日本学術振興会特別研究員 (DC2) 後, CYBERDYNE(株) 研究員. 人が道具へ適応する認知機能をテーマに, 現在装着型ロボットの安全技術の研究開発に従事. NEDO 生活支援ロボット実用化 PJ 業務管理者 (CYBERDYNE), ISO 13482 国内委員, IEC Expert. 日本ロボット学会研究奨励賞, IROS Conference Best Reviewer Award 等受賞. (日本ロボット学会正会員)

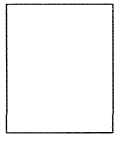

新宮正弘 (Masahiro Shingu)

2011 年筑波大学大学院システム情報工学研究科及び GCOE サイバニクス専修プログラム修了. 博士 (工学). CYBERDYNE(株) 研究員. サイバニクス技術を用いた神経-筋疾患患者の運動機能支援をテーマに, 人支援技術の研究開発・安全技術開発に従事. ISO 13482 国内委員. 日本機械学会等の会員. (日本ロボット学会正会員)

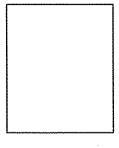

河本浩明 (Hiroaki Kawamoto)

2004 年筑波大学大学院システム情報工学研究科博士課程修了. 博士 (工学). 2005 年医療機器センター厚労科研リサーチレジデントを経て, 2008 年より筑波大学システム情報工学研究科助教. 2011 年より同学システム情報系助教. 人支援型ロボット, 生体運動制御に関する研究に従事. 日本機械学会等の会員. 日本ロボット学会論文賞受賞. (日本ロボット学会正会員)

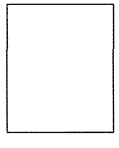

山海嘉之 (Yoshiyuki Sankai)

1987 年筑波大学大学院工学研究科修了. 工学博士取得後, 日本学術振興会特別研究員, 筑波大学機能工学系助手, 講師, 助教授, 米国 Baylor 医科大学客員教授. 2003 年より筑波大学大学院システム情報工学研究科教授. 2012 年より同学システム情報系教授. 新学術領域【サイバニクス】を開拓, 推進中. G-COE サイバニクス国際拠点リーダー, FIRST サイバニクス拠点統括者. 全国発明表彰大賞受賞. (日本ロボット学会正会員)

PLOS ONE

Long-Term Culture of Rat Hippocampal Neurons at Low Density in Serum-Free Medium: Combination of the Sandwich Culture Technique with the Three-Dimensional Nanofibrous Hydrogel PuraMatrix

Ai Kaneko*, Yoshiyuki Sankai

Center for Cybernics Research, University of Tsukuba, Tsukuba, Japan

Abstract

The primary culture of neuronal cells plays an important role in neuroscience. There has long been a need for methods enabling the long-term culture of primary neurons at low density, in defined serum-free medium. However, the lower the cell density, the more difficult it is to maintain the cells in culture. Therefore, we aimed to develop a method for long-term culture of neurons at low density, in serum-free medium, without the need for a glial feeder layer. Here, we describe the work leading to our determination of a protocol for long-term (>2 months) primary culture of rat hippocampal neurons in serum-free medium at the low density of 3×10^4 cells/mL (8.9×10^3 cells/cm^2) without a glial feeder layer. Neurons were cultured on a three-dimensional nanofibrous hydrogel, PuraMatrix, and sandwiched under a coverslip to reproduce the *in vivo* environment, including the three-dimensional extracellular matrix, low-oxygen conditions, and exposure to concentrated paracrine factors. We examined the effects of varying PuraMatrix concentrations, the timing and presence or absence of a coverslip, the timing of neuronal isolation from embryos, cell density at plating, medium components, and changing the medium or not on parameters such as developmental pattern, cell viability, neuronal ratio, and neurite length. Using our method of combining the sandwich culture technique with PuraMatrix in Neurobasal medium/B27/L-glutamine for primary neuron culture, we achieved longer neurites (≥3,000 μm), greater cell viability (≥30%) for 2 months, and uniform culture across the wells. We also achieved an average neuronal ratio of 97%, showing a nearly pure culture of neurons without astrocytes. Our method is considerably better than techniques for the primary culture of neurons, and eliminates the need for a glial feeder layer. It also exhibits continued support for axonal elongation and synaptic activity for long periods (>6 weeks).

Citation: Kaneko A, Sankai Y (2014) Long-Term Culture of Rat Hippocampal Neurons at Low Density in Serum-Free Medium: Combination of the Sandwich Culture Technique with the Three-Dimensional Nanofibrous Hydrogel PuraMatrix. PLoS ONE 9(7): e102703. doi:10.1371/journal.pone.0102703

Editor: Kari Hoyt, Ohio State University, United States of America

Received January 28, 2014; **Accepted** June 23, 2014; **Published** July 17, 2014

Funding: This study was supported by the Center for Cybernics Research (CCR) - World Leading Human-Assistive Technology Supporting a Long-Lived and Healthy Society granted by the Funding Program for World-Leading Innovative R&D on Science and Technology (FIRST Program, http://www.jsps.go.jp/english/e-first/first_reinforcement.html) initiated by the Council for Science and Technology Policy (CSTP). The funders had no role in study design, data collection and analysis, decision to publish, or preparation of the manuscript.

Competing Interests: The authors have declared that no competing interests exist.

* Email: kaneko@ccr.tsukuba.ac.jp

Introduction

The primary culture of neuronal cells plays an important role in neuroscience, especially in studies of their differentiation, nutritional requirements, and synapse formation. The ability to culture hippocampal neurons for 3–5 weeks, to allow them to become polarized and mature, extend axons and dendrites, and form synaptic connections, would be an extremely useful tool. For research on individual neurons or subcellular components, neurons should be plated at low density and maintained with a chemically defined medium because undefined components, such as serum, make it difficult to evaluate what factors are influencing neuronal growth. There has long been a need for methods enabling the long-term culture of primary neurons at low density in defined, serum-free, medium [1,2,3,4].

However, the lower the cell density, the more difficult it is to maintain the cultures of primary neurons in serum-free medium. Neuronal death at low density is caused by a lack of paracrine trophic support from adjacent neurons and glia [1]. When plated at low density (≤10^4 cells/cm^2), rat primary neurons from hippocampi or other brain regions typically die within days, suggesting that neuronal survival is critically dependent on their density (around 10^4 cells/cm^2) [5,6,7,8,9,4,10].

Co-culture of primary neurons with glial cells is often used to support neuronal survival [6,7,5,11,1,3,12]. However, much like serum, glial cells are also an undefined experimental variable. Although Neurobasal medium (Gibco, Life Technologies, Carlsbad, CA, USA) supplemented with B27 and L-glutamine is suitable for long-term culture of primary neurons at high density (≥1.6×10^4 cells/cm^2) [8], even these methods barely support the primary culture of neurons at low densities (≤10^4 cells/cm^2) for 1 month or more, which is still longer than other methods without a glial feeder layer [5,6,7,1,8,12,13]. At densities ≤10^4 cells/cm^2, cell viability or neurite bearing ratio is drastically decreased to 20–40% within 1 week after plating, whereas with a greater density, viability can be maintained at a high level (50–100%) [4,5,6,7,8,9,10,14,11,15,16].

In vivo, cells grow on a three-dimensional (3D) extracellular matrix (ECM), which provides a rough and large surface of nanofibers; hence, cells grown *in vitro* should also prefer to be cultured on 3D nanofibrous scaffolds [17]. Most cells in 2D culture, especially neurons, grow, react, differentiate, mature and die differently than cells *in vivo*. Many stem cells including induced pluripotent stem cells and embryonic stem cells can differentiate normally into neurons only in 3D culture. The 3D nanofibrous hydrogel PuraMatrix (BD Biosciences, Franklin Lakes, NJ, USA) is a peptide scaffold that self-assembles into nanofibers of 7–10 nm in diameter, similar to those comprising the ECM *in vivo*. A number of studies have used PuraMatrix hydrogel as a scaffold for primary neurons or the rat PC12 adrenal pheochromocytoma cell line [18,19]. This hydrogel was found to be more biocompatible than other scaffolds, such as Matrigel, and while 100% PuraMatrix decreased the viability of human neural stem cells, 25% PuraMatrix allowed their normal differentiation [20].

Low-oxygen conditions should also be replicated *in vitro* because the oxygen concentration *in vivo* is lower than that in air [21,22]. In an effort to experimentally replicate low-oxygen conditions, the sandwich culture method was first reported [4], and it is often used in co-culture with glial cells. For many applications and investigations, it is very important that primary neurons be cultured under conditions that resemble the *in vivo* environment as closely as possible, especially if the researcher is aiming to determine how neurons behave *in vivo*.

In the present study, we cultured rat hippocampal neurons using the sandwich culture technique in combination with PuraMatrix hydrogel to reproduce *in vivo*-like conditions, and we achieved long-term culture (>2 months). This is the first report of this combination, which has the potential for wide application in neuroscience research. Low-density (<10^4 cells/cm^2) neurons were plated on 3D PuraMatrix hydrogel, sandwiched under a coverslip, and cultured in Neurobasal medium. The neurons were exposed to concentrated paracrine factors under low-oxygen, microgradients of oxygen and other components, or different microenvironmental conditions. We assessed the viability of neurons and measured neurite length to determine the best culture conditions for replicating the *in vivo* situation. This determination of *in vivo*-like culture conditions in which neurites or axons extend over long distances may be beneficial not only to fundamental neuroscience research, but also to clinical applications in regenerative medicine because central nervous system (CNS) neurons and axons demonstrate a poor regenerative capacity. Long neurites on PuraMatrix can be considered an indicator of *in vivo*-like conditions, because neurite elongation is promoted by an *in vivo*-like collagen gel [23].

Materials and Methods

Ethics statements

All procedures with live animals conformed to the ethical guidelines established by the Japanese Council on Animal Care and were approved by the animal care committee of the University of Tsukuba (Permit Number: 11-324, 12-274).

3D hydrogel

To determine the best concentration of PuraMatrix to use in the present study, we tested three concentrations (100%, 50%, and 25%) in a preliminary experiment using neuronal-like PC12 cells. These concentrations were selected because the normal protocol for PuraMatrix recommends a concentration range of 25–100%. The longest neurites on PC12 cells and primary neurons were observed when cultured on the 25% PuraMatrix, which was therefore used for all subsequent studies.

PuraMatrix at a concentration of 25% was prepared by dilution with tissue culture water (Sigma-Aldrich, St. Louis, MO, USA) at a ratio of 1:3. Next, 0.5 mL of 25% PuraMatrix was carefully dispensed along the sidewalls of the wells of a 12-well tissue culture-treated multiplate (353043, BD Biosciences), after which 1 mL of culture medium was carefully added to induce gelation. The multiplate was placed in a 5% CO_2 incubator for 30 min to complete gelation. Subsequently, the medium was changed carefully two to three times over a period of 1 h to equilibrate the growth environment to physiological pH from its original pH of 2–4.

PC12 cell culture

PC12 cells were purchased from DS Pharma Biomedical Co., Ltd. (Osaka, Japan) and maintained in RPMI 1640 medium (Wako, Osaka, Japan) supplemented with 10% horse serum (Gibco) and 5% fetal bovine serum (FBS, Equitech-Bio, Inc., Kerrville, TX, USA) in tissue culture flasks (Primaria, BD Biosciences). Cells were dissociated by pipetting and plated on 12-well multiplates with or without PuraMatrix equilibrated with culture medium as described above. Immediately or 1 day after plating, nerve growth factor (NGF, 50 ng/mL in medium; BD Biosciences) was added to the cells to induce neuron-like differentiation. Cell morphology and neurite length were observed using an inverted microscope (Ti-S, Nikon, Tokyo, Japan).

Dissection and dissociation of primary hippocampal neurons

Hippocampal neurons were isolated from Wistar rat embryos on embryonic day 18 (E18) or E19. The hippocampi of E18–19 rats are homogenously composed of major pyramidal neurons and a few glial cells, and are generally used as a source of primary neurons [3]. Pregnant female Wistar rats were purchased from SLC (Shizuoka, Japan).

Approximately 10 fetuses were obtained from each rat, and whole brains were isolated from the fetuses. About 20 hippocampi were dissected from the brains under a stereoscopic microscope using two pairs of fine tweezers. The meninges were carefully removed from the hippocampi. All fetuses and tissues were maintained in minimum essential medium (MEM, Sigma) and chilled on ice. All subsequent procedures except for incubation and centrifugation were performed in a laminar flow hood.

After dissection, the hippocampi were washed gently with 7–8 mL of phosphate-buffered saline (PBS, Wako) in a 15-mL conical tube three times. After washing, 5 mL of a papain solution and 20–60 μL of deoxyribonuclease I (DNase I, 5 units/μL, Takara, Shiga, Japan) were added to the hippocampi in the tube, which were then incubated at 32°C for 12 min. The papain solution was prepared by dissolving 70 mg of papain (0.5 units/g, Wako) and 10 mg of ethylenediamine tetraacetic acid-2Na (Wako) in PBS to a final volume of 20 mL. The papain solution was filtered using a 0.2-μm filter (Sartorius, Gottingen, Germany), divided into 5 mL aliquots, and stored at −30°C. The papain solution was thawed slowly at 4°C for several hours before use.

After incubation and digestion with the enzymes, hippocampi were slowly pipetted using a glass Pasteur pipette 12 times, and then filtered using a wetted cell strainer (40-μm mesh, BD Biosciences) into a 50-mL conical tube. The cell strainer was previously wetted with 10 mL of MEM (Sigma) containing 20% FBS (Gibco) and 1% N2 supplement (100×, Invitrogen, Life

Technologies) to prevent nonspecific neuronal cell attachment. The entire hippocampi suspension was poured through the cell strainer, and then 10 mL of 20% FBS/N2/MEM was poured on top to collect neurons remaining on the filter. The total volume of 25 mL was shaken gently to inactivate enzymes, left for 1 min, and then centrifuged at 180×*g* for 10 min. Next, the supernatant was aspirated, and the pellet was resuspended in the culture medium described below at a constant cell density of 3×10^4 cells/mL. This density corresponded to 8.9×10^3 cells/cm^2 in the 12-well multiplates (culture area: 3.38 cm^2). Subsequently, the cell suspension was plated into the wells of 12-well multiplates in a volume of 1 mL per well. Each well had been previously prepared with 0.5 mL of 25% PuraMatrix, so plating was performed gently. Rat embryonic hippocampal neurons prepared in this way were cultured at 37°C in a humidified atmosphere with 5% CO_2/95% air.

Culture medium

The basic culture medium used in the present study was Neurobasal medium (Gibco) containing 2% B27 supplement (50×, Invitrogen) and 0.5 mM L-glutamine (Wako), which is described as medium #0 throughout this article. Extra supplements were added to basic medium #0 as described below, according to the manufacturer's protocol for Neurobasal medium.

Medium #1: 0.5 mM GlutaMAX I (Invitrogen), which is L-alanyl-L-glutamine and a dipeptide substitute for L-glutamine, was added to medium #0 in place of L-glutamine. Because this supplement breaks down slowly, medium #0 was used as the plating medium, and #1 was used after the first medium change. The protocol for GlutaMAX indicates that it may reduce or remove the need for medium changes. To verify this, we also examined an experimental group wherein the medium was changed only the first three times.

Medium #2: 25 µM L-glutamic acid (Sigma) was added to medium #0 [9]. Medium #2 was used only during plating to prevent toxicity from glutamic acid. After the first medium change, medium #0 was used. In some cases, medium #1 was used after the first medium change, which is described as #2/1.

Medium #3: 25 µM 2-mercaptoethanol (Gibco) was added to medium #0 [24,25]. This thiol works as a reducing agent, and may replicate *in vivo* conditions, where low oxygen causes reduction of many chemical substances.

For comparison with basic medium #0, Dulbecco's Modified Eagle's Medium/Ham's Nutrient Mixture F-12 (DMEM/F12, Invitrogen) and MEM media were also used. DMEM/F12 was supplemented with 0.1% bovine serum albumin (BSA, Sigma), 5 ng/mL brain-derived neurotrophic factor (R&D Systems Inc., Minneapolis, MN, USA), 1% N2 (50×, Invitrogen), and 2% B27 (Invitrogen). MEM was supplemented with 2% FBS and 1% N2 as a low serum medium.

For changes of Neurobasal medium-containing media, mediums #0–#3, half of the medium (0.5 mL per well) was exchanged twice a week. For changes of DMEM/F12 medium, 25% of the medium (0.25 mL per well) was exchanged twice a week. Medium changes were done gently so as not to break the PuraMatrix hydrogel or disrupt neuronal attachment or neurite extension.

Sandwich culture of primary neurons using PuraMatrix and coverslips

Neuronal cell suspensions prepared as described above were plated on PuraMatrix after equilibration. Thereafter, the neurons were incubated at 37°C in a humidified 5% CO_2/95% air atmosphere. Approximately 3 h after plating, the neurons had adhered to the PuraMatrix, and were covered with a sterilized round glass coverslip (18 mm in diameter, Matsunami, Osaka, Japan). To determine the best time to cover the cells, three different time points were tested: 1, 3, and 22 h after plating.

Statistical analysis of neurite length and viability

The suitability of different culture conditions was evaluated based on cell viability and neurite length. Viability is a direct indicator of the possibility of long-term cell culture, and neurite length is an indicator of neuronal growth, differentiation, and maturation. In many studies, neurite length is used as an indicator of normal morphogenesis, gene expression, or molecular dynamics [12,7,18,25,26,23].

Neurite length was measured by phase-contrast imaging using a Nikon inverted microscope, mainly with the 20× objective. Neurite lengths were calculated from digital images using their scale bars. Neurite length was measured using a standard technique for measuring the curve length: the neurite curve was approximated by multiple straight line segments, and the lengths of these line segments were added together [27]. For statistical analysis, the five longest neurites in each well were selected [26]. Because it was difficult to trace the lengths of neurites growing on the very rough surface of PuraMatrix, they were excluded from the final analysis. Some neurites overlapped or crossed other neurons or neurites; these overlapping regions were observed at higher magnification (60× objective) to check neurite continuity.

Viability was judged by phase-contrast microscopy using the 20× objective on a Nikon inverted microscope. Viability was calculated from the number of living cells with bright, round, and smooth soma and extended neurites. The initial number of living cells per photographed area was counted directly several hours after plating, or calculated from three values: plating density, well area, and photographed area. The living cell number was counted on each observation day and the ratio of the living cell number to the initial number at plating was used for analysis.

Comparisons between different groups with different culture conditions were performed using Student's t-tests. The maximum neurite lengths were measured from the five longest neurites in each well on phase-contrast images. Similarly, 5–6 images from different areas in each well were taken to count living cells for cell viability. To study differences in position, three photographs were taken at both the center and the edge of each well.

In order to determine the best culture conditions, experiments were repeated three or more times with different rats or batches of cells. From these replicates, the means and standard errors of the maximum neurite length were calculated once or at several time points during the culture. Similarly, cell viabilities were calculated and compared between different culture conditions.

Statistical analysis by immunofluorescence staining

Cell viability and neurite length were measured using the LIVE/DEAD Viability/Cytotoxicity Kit (Molecular Probes, Eugene, OR, USA). Fluorescence images were taken using a fluorescence microscope (Ti-S, Nikon) with a triple band filter (4′,6-diamidino-2-phenylindole (DAPI)/fluorescein-5-isothiocyanate (FITC)/Texas red). By counting the numbers of green cells, cell viability was calculated, and by measuring the lengths of green neurites, neurite length was determined. Thus, viability and neurite length were assessed from fluorescence images, as well as from phase-contrast images.

Immunocytochemistry to determine the neuronal ratio

To distinguish neurons from astrocytes and determine the neuronal ratio, the cells were double-stained with anti-microtubule-associated protein 2 (MAP2) and anti-glial fibrillary acidic protein (GFAP). For immunostaining, cultured cells in a well were washed with 37°C PBS and fixed with 4% paraformaldehyde for 20 min. After washing with 37°C PBS, the fixed cells were permeabilized with 0.1% Triton-X in PBS for 5 min. Following two washes with PBS, the cells were blocked with 10% goat serum in PBS at 37°C for 30 min. Next, the following antibodies were applied: mouse monoclonal anti-MAP2 (1:50, Sigma) for neurons, and rabbit polyclonal anti-GFAP (1:400, Dako, Glostrup, Denmark) for astrocytes. The cells were incubated with the primary antibodies in blocking buffer at 37°C for 1–2 h. After washing, the following secondary antibodies were applied: Alexa Fluor 488 goat anti-mouse immunoglobulin G (IgG) (1:100, Molecular Probes) and Alexa Fluor 594 goat anti-rabbit IgG (1:100, Molecular Probes). The cells were incubated with the secondary antibodies in blocking buffer at 37°C for 30 min. After washing with PBS and removing the coverslip, if applicable, the cells were mounted with Vectashield mounting medium for fluorescence with DAPI (Vector Laboratories, Burlingame, CA, USA) to counterstain the nuclei. Fluorescence images were obtained using a Nikon Ti-S microscope with a triple band filter (DAPI/FITC/Texas red).

The neuronal ratio (%) was expressed as the percentage of the total cells (i.e. neurons plus astrocytes) made up by neurons. Cell numbers were counted at six positions: three in the center of the well and three at its edge. The total numbers of neurons and astrocytes in each well were used for analysis.

Synapse activity

To study synapse formation and activity after long-term culture, neurons on PuraMatrix covered by a coverslip were stained with the synaptic vesicle marker FM1-43 (Molecular Probes). A working solution of 20 µg/mL dye was prepared in ice-cold Hank's balanced salt solution for staining. The culture medium was removed from cultured neurons on PuraMatrix after 49 days *in vitro* (DIV), and the staining solution was added to the well. After 1 minute, when recycling synaptic vesicles should have already been stained, the staining solution was removed and the culture medium was replaced to reduce background and non-specific adsorption of the working solution. After removing the coverslip, the stained neurons were observed. Phase contrast images and green fluorescent images were obtained using Ti-S (Nikon) and BZ-9000 (Keyence, Osaka, Japan) microscopes. The BZ-9000 microscope has many specialized functions, such as haze reduction and background adjustment. We used the BZ-9000 microscope to obtain high-resolution images with low background because the PuraMatrix, 3D hydrogel tends to cause non-specific adsorption of dye, high background, low resolution, and unfocused images.

Ultrastructural analysis of PuraMatrix

To analyze the ultrastructure of PuraMatrix during primary culture, we used a digital microscope (VHX2000/1100, Keyence) that can take 3D optical images non-destructively. It is important to study the surface roughness of PuraMatrix during culture with living neurons in culture medium. We examined PuraMatrix ultrastructure in two different wells using a digital microscope, and obtained similar results. Two kinds of 3D images were examined: color 3D images with 2D cross-sectional profiles, and high contrast 3D images using the high dynamic range function, which is useful for transparent and low contrast surfaces.

Primary culture without PuraMatrix

To compare culture media under 2D culture conditions without coverslips or PuraMatrix, three kinds of media were used: 2% FBS/N2/MEM, DMEM/F12 medium, and basic medium #0. Primary neurons were plated at 3×10^4 cells/mL into 2D culture vessels, 35-mm glass bottom dishes (Advanced TC, Greiner Bio-One GmbH, Frickenhausen, Germany), and 12-well multiplates (Advanced TC, Greiner Bio-One). The growth area of these vessels was surface-modified for cell culture, primary cell culture in particular.

Results

PC12 cells and PuraMatrix

Before primary neuron culture, the best concentration of PuraMatrix was determined using PC12 cells. When plated on PuraMatrix, PC12 cells adhered within several hours, extended neurites by the next day, and sometimes those neurites extended > 1,000 µm. Without PuraMatrix, PC12 cells aggregated in solution, but did not attach to the bottom of the well or extend neurites. The effects of PuraMatrix concentration and cell density on neurite length were studied (Table 1). PC12 cells were plated at three different cell densities, 3×10^2, 3×10^3, and 3×10^4 cells/mL, all of which were tested on PuraMatrix at concentrations of 25%, 50%, and 100%. The maximum neurite length, calculated from the three longest neurites at DIV 23, was 1,000±58 µm (mean ± SE, n = 3) on 25% PuraMatrix, significantly higher ($P<0.05$) than that (around 600 µm) on 50% or 100% PuraMatrix. At 3×10^4 cells/mL, such long neurites were only rarely distinguishable because the cells had aggregated.

Primary neurons cultured on 25% and 50% PuraMatrix were also compared. The maximum neurite length calculated from the four longest neurites at DIV 3–4 was 340±39 µm (mean ± SE, n = 4) on 25% PuraMatrix, significantly higher ($P<0.05$) than that (188±40 µm) on 50% PuraMatrix. Based on these results and those of a previous study [20], 25% PuraMatrix was selected for all subsequent primary culture experiments.

Developmental pattern of rat hippocampal primary neurons

Using our combination method, neuronal cells were sandwiched between the PuraMatrix and a coverslip. Surface roughness, or the variation in height of the 25% PuraMatrix in the culture condition, was determined using the digital microscope (VHX2000/1100, Keyence) to be typically 10–20 µm, and 40 µm at the maximum (Fig. 1).

The effects of the 3D PuraMatrix hydrogel and coverslip on primary cultured neurons were evaluated by measuring neurite length, cell viability, and neuronal ratio. In addition, various cell densities, medium components, medium change, embryonic days for dissociation of the hippocampus, and the timing of the coverslip placement on top of the hydrogel were tested (Table 1). We selected neurite length as a parameter for assessing culture conditions because it is an indicator of whether many neurons survive, differentiate, and mature. Indeed, axons elongate 5–10 times faster than dendrites, and longer neurites are considered to be differentiated axons at maturation stage 5 [12]. We found measurements of spine density or factors other than neurite length to be relatively inaccurate and difficult compared with measuring neurite length because the resolution of neuronal images is decreased by the rough, thick, and semi-opaque 3D PuraMatrix. In addition, it is difficult to achieve proper focus on structures as small as spines on a rough surface. Axons could be measured more simply than any other structure.

The developmental pattern of primary neurons in the best culture conditions as determined in the experiments described below is shown in Figure 2. After plating onto 12-well multiplates prepared with 25% PuraMatrix, the neurons attached and started

Table 1. Summary of the culture conditions tested and the best culture conditions in each case.

Experiment No.	Cell type	PuraMatrix	Cell density [cells/mL]	Medium and medium change (+/−)*	Coverslipping [h after plating]	Best culture conditions for neurite extension over long distances and maximum neurite length
1	PC12	25/50/100%	3×10^2, 3×10^3, 3×10^4	RPMI 1640/10% horse serum/5% FBS (+), NGF+	–	25% PuraMatrix at 3×10^2 and 3×10^3 cells/mL, 1,000±58 μm (n = 3)
2	E18	25/50%	10^3, 10^4, 10^5	DMEM/F12 medium (+), 2% FBS/N2/MEM (+)	–	25% PuraMatrix, DMEM/F12 medium (+), at 10^4 cells/mL, 340±39 μm (n = 4)
3	E18/E19	25%	3×10^3, $1–1.25\times10^4$, $2.5–3\times10^4$, 10^5	#0 (+/−), DMEM/F12 \medium (+/−)	–	#0 (+) at $2.5–3\times10^4$ cells/mL, 1,600±460 μm (n = 4)
4	E18/E19	25%	$2.5–3\times10^4$	#0 (+), DMEM/F12 medium (+)	–	E18, #0 (+), 1,800±586 μm (n = 3)
5	E18	25%	3×10^4	#0 (+)	−/1/3/22	3 h coverslipping, around 1,800 μm
6	E18	25%	3×10^4	#0 (+), #1 (+/−), #2 (+), #2/1 (+), #3 (+), DMEM/F12 (+), 2% FBS/N2/MEM (+)	−/3	#0 (+) or #2 (+), 3 h coverslipping, >2,000 μm
7	E18	None	3×10^4	#0 (+), DMEM/F12 medium (+), 2% FBS/N2/MEM (+)	–	#0 (+), several hundred micrometers
8	E18	25%/None	3×10^4	#0 (+)	−/3	25% PuraMatrix, 3 h coverslipping, ≥3,000 μm

Data are shown as mean ± SEM for sample size n.
The best culture conditions were determined in experiments 1–7, and then a conclusive experiment 8 was performed.
E18, E19: Primary neurons isolated from rat fetal hippocampi on embryonic days 18 and 19.
*medium change (+): medium changes.
*medium change (−): no medium changes.
*For medium name, see "Culture medium" section.
doi:10.1371/journal.pone.0102703.t001

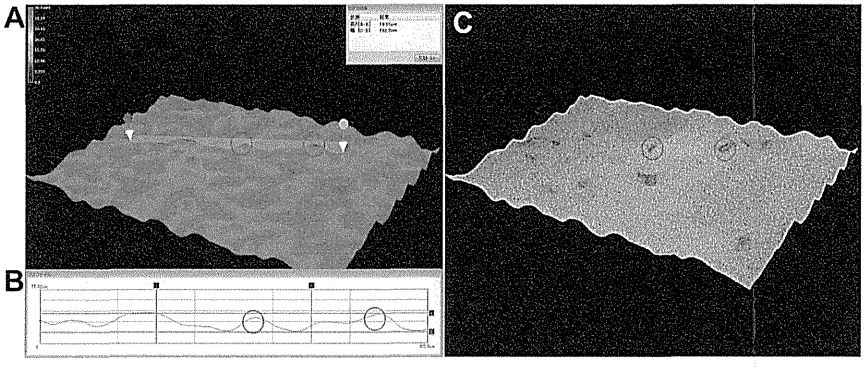

Figure 1. Three-dimensional images of the surface roughness of PuraMatrix with adherent neurons observed using a digital microscope. The neurons were cultured on 25% PuraMatrix in basic medium #0 for 1 month. Two neurons are shown by red circles. (A) Color 3D image. The highest positions are displayed in red and the lowest positions in blue (see color scale at the upper left). The maximum height difference was <40 μm. (B) Cross-sectional profile between the two arrows in A showing a height of 19.32 μm (A–B) and a width of 455.8 μm (C–D: 182.3 μm). The neurons and PuraMatrix show a typical height difference, or surface roughness, of approximately 10–20 μm. (C) High contrast 3D image using the high dynamic range function. The transparent neurons are emphasized by their dark color.
doi:10.1371/journal.pone.0102703.g001

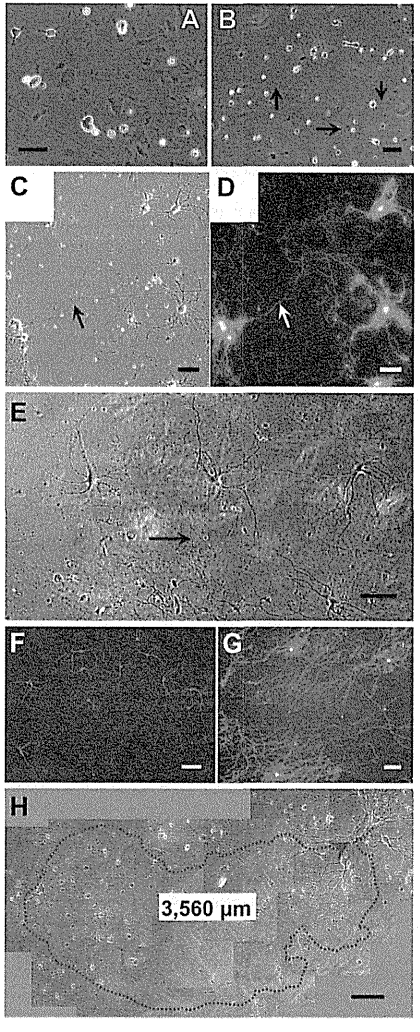

Figure 2. Developmental pattern of primary neurons plated on 25% PuraMatrix at 3×10^4 cells/mL. The neurons were isolated from the hippocampi of embryonic rats (E18) and cultured in basic medium #0 or #2 (E, H). A coverslip was placed over the neurons 3 h after plating. Bars: 50 μm or 100 μm (E–H). (A) Phase-contrast image of neurons 3 h after plating. The neurons attached to PuraMatrix, and extended lamellae or short neurites within 50 μm. (B) Phase-contrast image of neurons at DIV 1. The neurons started to extend one neurite that was several times longer than the others. The long neurites (arrows, approximately 300 μm) are assumed to be axons, and the other, shorter ones, dendrites. (C) Phase-contrast image of neurons at DIV 21. The neurons extended neurites for several hundred microns (axons, arrow), as well as neurites with branches and spines (dendrites). Axons and dendrites formed fine networks. (D) Fluorescence image of (C), stained with the LIVE/DEAD Viability/Cytotoxicity Kit. Living cells and neurites are stained green, dead cells red. (E) Phase-contrast image of neurons at DIV 36. The neuronal cell bodies are increased in size. Dendrites have characteristic spines that are increased in length, tapered and branched. Axons (arrow) show a uniform diameter over a long distance. The neurons formed neuronal networks and matured. (F) Fluorescence image of neurons at DIV 38. Neurons and astrocytes are double-stained with anti-MAP2 for neurons (green) and anti-GFAP for astrocytes (red), with DAPI as a nuclear counterstain (blue). Neuronal survival for 5 weeks without glial proliferation is shown. (G) Fluorescence image of neurons at DIV 42, stained with the LIVE/DEAD Viability/Cytotoxicity Kit. Neuronal survival and neurite extension is shown. (H) Phase-contrast image of neurons at DIV 63. The neurons show bright, round, and smooth somas, and long axons of a uniform diameter (3,560 μm, arrow), suggesting their survival for 2 months.
doi:10.1371/journal.pone.0102703.g002

to extend neurites within 3 h (Fig. 2A), showing characteristics of developmental stages 1 or 2 [12]. Three hours after plating, a coverslip was placed on the neurons in each well. Within several days, the neurons started to extend one neurite that was longer than the others, showing characteristics of developmental stage 3 (Fig. 2B, arrows). Subsequently, the neurons extended these neurites over several hundred microns (now assumed to be axons, arrows in Fig. 2C–D), as well as neurites with branches and spines (dendrites), showing characteristics of developmental stages 4 or 5. Such identification of axons and dendrites based on their length and morphology agrees with immunoreactive staining against MAP2, a protein specific to dendrites [12]. Thus, the neurons differentiated, maturated to developmental stage 5, extended axons (≥3,000 μm), and survived long-term for over 2 months without glial proliferation (Fig. 2E–H). In addition, the neurons continued to maintain fine neuronal networks with a single-cell distribution, i.e., the distances between the neurons were maintained well.

Assessment of best cell density and medium change

The best cell density and medium change procedures were examined using DMEM/F12 medium and Neurobasal medium/B27/L-glutamine (basic medium #0 as described in "Culture medium" section). Before examining the effects and timing of coverslip placing, we looked at the effects of media type and medium changing, cell density, and embryonic day, because these conditions had greater effects on neuronal growth (i.e., they altered neurite length severalfold).

Media were changed as described in "Culture medium" section (+), or left unchanged (−) for comparison. Cell density was 3×10^3, $1–1.25\times10^4$, $2.5–3\times10^4$, or 10^5 cells/mL. For each condition, the maximum neurite length during culture was measured as an indicator of neuronal survival and active outgrowth without regression. Experiments were repeated three to five times with different rats or batches of cells. The maximum neurite lengths were highest in medium #0 (+) at $2.5–3\times10^4$ cells/mL, 1,600±460 μm (mean ± SE, n = 4), although the differences between most groups in medium #0 were not significant. Compared with this condition, neurite lengths in DMEM/F12 medium were significantly shorter (approximately 500 μm, $P<0.05$) for all conditions. Based on these results, the best culture conditions were determined to be a cell density of 3×10^4 cells/mL

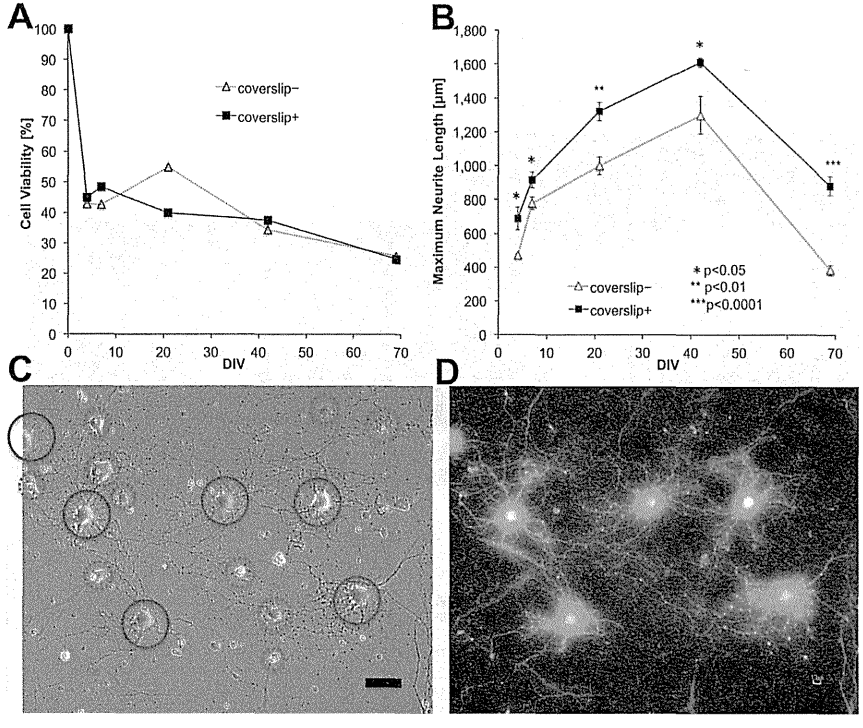

Figure 3. Effect of the coverslip on cell viability and maximum neurite length of primary neurons. Neurons from E18 rat hippocampi were plated on 25% PuraMatrix at 3×10^4 cells/mL in basic medium #0, and coverslipped 3 h after plating (+), or not (−). The neurons were plated into five multiplates simultaneously, and the cell viability and neurite length in one plate were examined only once at DIV 4, 7, 21, 42, or 69. (A) Cell viability calculated from the mean of two wells. Cell viability was evaluated by phase-contrast microscopy, and is expressed as the fraction of the living cell number 3.5 h after plating (DIV 0, 100%). Living cell numbers were counted in six areas for each well: three areas in the center and three areas at the edge of the well. There were no significant differences between coverslip (+) and (−) conditions in any of the 12 sets of data from the two wells (two-tailed Student's t-test). (B) The maximum neurite length was expressed as the mean and standard error from the five longest neurites in each well stained with the LIVE/DEAD Viability/Cytotoxicity Kit. For each pair of coverslip (+) and (−) treatments at each DIV, significant differences are shown (one-tailed Student's t-test). The maximum neurite length in the coverslip+ condition was significantly longer than that in the coverslip− condition throughout the culture period of DIV 4–69. (C) Phase-contrast image of coverslip+ neurons at DIV 21. Bar: 50 µm. (D) Fluorescence image of (C) stained with calcein AM (green) and ethidium homodimer-1 (red). Living cells and neurites are stained green, shown as the bright, smooth cells in C (green circles). Dead cells are stained red, shown as rough or dark cells in C (red circles). C and D show that approximately 40% of the neurons attached to PuraMatrix were alive at DIV 21 and had extended neurites and formed neuronal networks.
doi:10.1371/journal.pone.0102703.g003

(8.9×10^3 cells/cm^2) in basic culture medium #0 with medium changes.

Assessment of embryonic day for isolation of hippocampal neurons

Primary neurons were isolated from rat fetal hippocampi on E18 and E19. Neurons were plated on 25% PuraMatrix at a cell density of $2.5–3\times10^4$ cells/mL. Basic medium #0 and DMEM/F12 were used and compared. Neurite length was measured at least once a week, and the maximum value during culture was used for analysis. Experiments were repeated three times with different batches of cells. Neurite length was highest with neurons isolated from E18 hippocampi and cultured in medium #0, 1,800±586 µm (mean ± SE, n = 3), and this length was more than twice that found in E19 hippocampal neurons in medium #0 (833±88 µm). The neurite lengths of cells cultured in DMEM/F12 medium were approximately 500 µm, 490±26 µm for E18 and 497±33 µm for E19 hippocampi. Based on this result, hippocampal neurons from E18 embryos were cultured in medium #0 for all subsequent experiments because this condition provided more than twice the neurite lengths of all the other conditions, though these differences were not significant.

Timing of coverslip placement

To determine the best timing for coverslip placement on neuronal cells, three different time points were tested: 1, 3, and 22 h after plating of neurons. Cultures without coverslips were also tested. Neurons isolated from E18 embryos were plated on PuraMatrix and cultured in basic culture medium #0 with medium changes as described above. Experiments were repeated three or four times for each time point with cells from different rats. For statistical analysis, means and standard errors of cell viability and maximum neurite length were measured four to six times during culture. Only a few significant differences in cell viability were found among the different coverslip placement times at each measurement point, and that the mean viabilities did not differ either. The maximum neurite lengths were highest with placement at 1 or 3 h when assessed at DIV 3–8, and highest with placement at 3 or 22 h when assessed at DIV 14–38. The maximum neurite lengths with coverslip placement at 3 h were significantly longer than in the other cases (1 h, 22 h, and without a coverslip) at nine time points (DIV 4–35) in all the 4 replicates, and significantly shorter than the 1 h placement at the early two time points (DIV 4, 8) in only one replicate. In addition, long neurites of approximately 1,800 µm were repeatedly obtained only with this coverslip placement timing.

The best time for coverslip placement was chosen as 3 h after plating because 3–5 weeks after plating is an extremely important period for neuronal research, and significantly longer neurites were found during that period only when using 3 h coverslip placement. Based on these results, coverslips were placed on cultured neurons 3 h after plating in all subsequent experiments.

Comparison of culture media

The best culture medium for primary neurons was determined using the media formulations described in the "Culture medium" section. Primary neurons were suspended in each medium, and then plated into two wells containing PuraMatrix for each medium. In one well for each medium, a coverslip was placed on the cultured neurons 3 h after plating as described above. The condition without a coverslip is hereafter described as medium−, and that with a coverslip is described as medium+. Experiments were repeated three to four times for each medium with cells from different rats. From these repetitions, means and standard errors of the maximum neurite length and cell viability were calculated at 2, 3, 5, and 8 weeks after plating.

The cell viabilities were not significantly different between medium+ and medium− conditions for each medium at 2, 3, 5, or 8 weeks. Cell viabilities in medium #0+ (around 30%) were not different from those in #1+, #2+, or #2/1+, all media composed of Neurobasal medium. However, viabilities in DMEM/F12+ (around 10% or lower) continued to be significantly lower than those in medium #0+.

The maximum neurite length in each medium+ was generally longer than that in each medium−, although there were no significant differences ($P<0.05$), except for #1 at 2 weeks and DMEM/F12 at 5 weeks. The maximum neurite lengths were highest (≧1,000 µm) with conditions #0+ and #2+, which were also longer overall at 3–8 weeks. In addition, extremely long neurites (>2,000 µm) were repeatedly obtained only when using the #0+ and #2+ conditions. However, neurite lengths in #0+ and those in #1+, #2+, or #2/1+ were not significantly different ($P<0.05$), except for #2/1+ at 3 weeks. Neurite lengths in DMEM/F12+ were significantly shorter (around 500 µm) than those in #0+ at 2–8 weeks.

No other media tested produced longer neurites or higher viabilities than media #0 and #2. In particular, low serum medium (2% FBS/N2/MEM) produced extremely short neurites (<100 µm).

Based on these results, #0+ (basic medium #0 with a coverslip) was selected for all subsequent experiments. Although condition #2+ produced a greater mean maximum neurite length, it often resulted in lower cell viability and larger variations in neurite length and viability. The cell viabilities in conditions #0+ and #2+ were 32±2% and 27±3% (mean ± SE, n = 4 for both) at 5 weeks, and 25±4% and 24±5% at 8 weeks, respectively. The maximum neurite lengths in conditions #0+ and #2+ were 1,271±148 µm and 1,374±289 µm at 5 weeks, and 1,032±78 µm and 1,132±345 µm at 8 weeks, respectively. For better stability and reproducibility in long-term culture, basic medium #0 was selected.

Finally, we evaluated the effect of medium alone with neither coverslip nor PuraMatrix. Primary neurons were plated into regular 2D culture vessels at 3×10^4 cells/mL, and cultured in three different media: 2% FBS/N2/MEM, DMEM/F12 medium, and basic medium #0. When plated onto glass bottom dishes, neurons died or released within several days in 2% FBS/N2/MEM or DMEM/F12 medium. In #0, however, they extended neurites of several hundred microns. When plated into 12-well multiplates, neurons showed similar results, though glial cells proliferated in 2% FBS/N2/MEM. With neither coverslip nor PuraMatrix, #0 achieved higher viability, longer neurites, and decreased proliferation of glial cells.

Effect of the coverslip

The effect of the coverslip was evaluated using the best culture conditions as described above (see Table 1): primary neurons were plated on 25% PuraMatrix, maintained in basic medium #0, half of the medium was changed twice a week, the cell density was 3×10^4 cells/mL, the neurons were isolated from E18 rat hippocampi, and a coverslip was placed on the neurons 3 h after plating (+) or not placed for comparison (−).

The experiments over 1–2 months were repeated 14 times with cells from different rats. Based on these repetitions, only a few significant differences in cell viability were found at each time point between coverslip (+) and (−) conditions, and the maximum neurite lengths were significantly longer in coverslip (+) than (−) conditions at one or more time points during DIV 4–60. The maximum neurite length in coverslip (+) condition typically became highest (1,100–1,700 µm) at DIV 24–60 during each repetition. There were significant differences in viabilities between coverslip (+) and (−) conditions at only four times among the 62 time points: viability was higher in coverslip (+) twice, and in coverslip (−) conditions twice as well. Microscopy was mostly performed four to six times to measure cell viability and neurite length, and the resulting values tended to become lower when microscopy was repeated several times before DIV 14. In 4 replicates, microscopy was performed once or not performed before DIV 14, resulting in 39±4% (mean ± SE, n = 4) viability at DIV 35 and 27±5% at DIV 53–60.

To prevent any potential effects of the microscopy and staining on neuron health, the following examinations were performed in 2 of the 14 replicates. Neurons were simultaneously plated into five multiwell plates, and the cell viability and neurite length were examined in one plate at each DIV. The cell viabilities were averaged from two wells as assessed by phase-contrast microscopy, and neurite length was assessed from one well by fluorescence

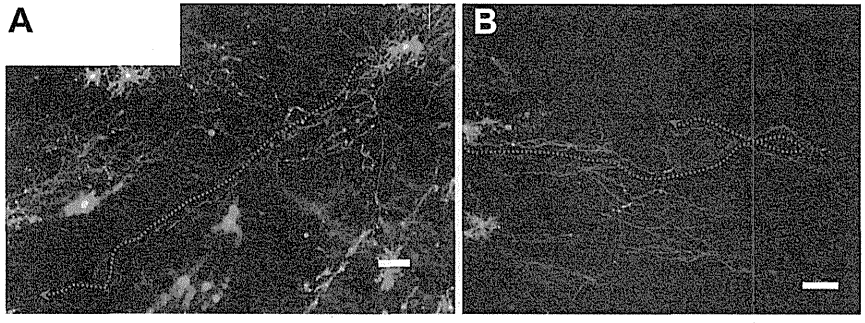

Figure 4. Fluorescence images showing long-term neuronal survival and long neurites at DIV 42 in Fig. 3. The primary neurons were plated on 25% PuraMatrix at 3×10^4 cells/mL, and coverslipped 3 h after plating (B), or not (A). Living cells and neurites are stained green with calcein AM, and dead cells red (dots) with ethidium homodimer-1. Bars: 100 μm. Both A and B show long neurites (>1,600 μm, arrows). As shown in (A), fluorescence images can be used to study the 3D growth of neurites because neurites on the rough surface of PuraMatrix can be traced by green fluorescence, even if they are out of focus.
doi:10.1371/journal.pone.0102703.g004

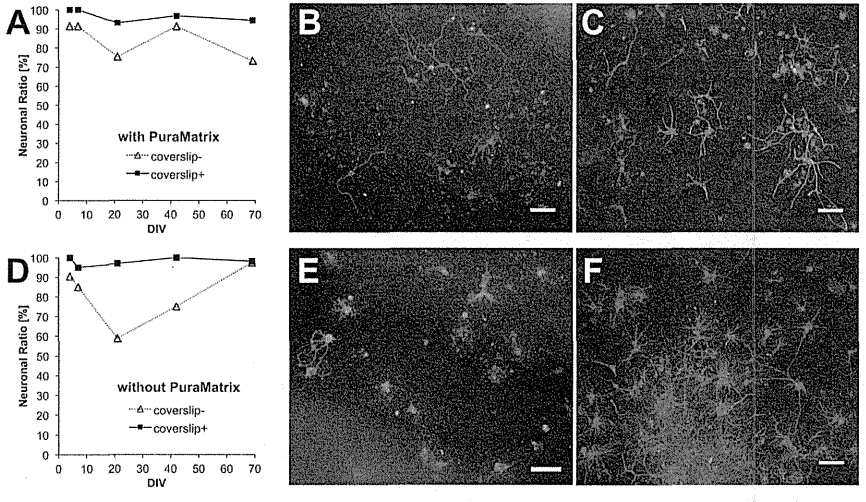

Figure 5. Effect of the coverslip and PuraMatrix on the neuronal ratio of primary neurons. Bars: 100 μm. Neurons from E18 rat hippocampi were plated at 3×10^4 cells/mL in basic medium #0 and coverslipped 3 h after plating (+), or not (−). Before plating, 25% PuraMatrix was already prepared in a well (A–C) or the wells were not treated (D–F). The neurons attached to PuraMatrix (A–C) or the polystyrene, tissue culture-treated bottom (D–F) and grew. The neurons were plated into five multiplates simultaneously, and the neuronal ratio in each plate was only examined once at DIV 4, 7, 21, 42, or 69. Neurons and astrocytes were double-stained with anti-MAP2 for neurons (green) and anti-GFAP for astrocytes (red), with DAPI as a nuclear counterstain (blue). Neurons and astrocytes were counted in six areas in each well: three areas in the center and three areas at the edge, and their total numbers were used for analysis. The neuronal ratio was consistently higher in the coverslip+ compared with the coverslip− condition at DIV 4–69 (A, D). (A) Our combined sandwich culture technique using both a coverslip and PuraMatrix (coverslip+) achieved a high neuronal ratio of nearly 100%. Fluorescence images at DIV 42 at the edge of the coverslip+ (B) and coverslip− (C) wells. (B) Neurons (green) preceded astrocytes (red). (C) Astrocytes proliferated locally, mainly at the edge of the well. (D) Sandwich culture using coverslip only (coverslip+) also yielded a high neuronal ratio of nearly 100%. Fluorescence images at DIV 42 at the edge of the coverslip+ (E) and in the center of the coverslip− (F) wells. (E) Neurons (green) preceded astrocytes (red). The image is unfocused because of the influence of intrinsic fluorescence of the polystyrene well itself, especially at the edge. (F) Astrocytes proliferated locally, mainly in the center of the well, where many cells aggregated.
doi:10.1371/journal.pone.0102703.g005

microscopy after staining using a LIVE/DEAD Viability/Cytotoxicity Kit. The viabilities and neurite lengths of these replicates were similar, and one replicate is shown in Figure 3. Cell viability was noticeably decreased within a few days after plating, and then continued to decrease in a linear and extremely gradual manner over DIV 7–69 (Fig. 3A). Viability was 40–50% at 3 weeks, approximately 40% at 6 weeks, and 30% at 2 months after plating. There was no significant difference in viability between conditions (+) and (−). These viabilities were as high as or higher than the 4 replicates mentioned above. At DIV 21, approximately 40% of neurons attached to the PuraMatrix were alive and stained green (Fig. 3D). The average viability at DIV 21 is shown in Figure 3C–D. There was no significant difference between the results determined by phase-contrast and fluorescence microscopy for both cell viability and maximum neurite length (Fig. 3C–D).

The maximum neurite length achieved in coverslip (+) was significantly longer than that in coverslip (−) at all time points examined (Fig. 3B). The difference was extreme at DIV 69 ($P<0.0001$), demonstrating the growth-promoting effect of the coverslip during long-term primary culture over 2 months. Our combination culture with a coverslip and PuraMatrix continued to yield long neurites: >800 μm at DIV 7–69 and >1,300 μm at DIV 21–42 (Figs. 3B, 4). The presence of long neurites (>1,600 μm) at DIV 42 is shown in Figure 4 (note that the density of living cells appears less here than in most of the other images taken to assess viability).

Neuronal ratio

To evaluate the effects of coverslip and PuraMatrix on the neuronal ratio, we studied four conditions (Table 1, Experiment 8): one with both PuraMatrix and a coverslip (our combination method); one with PuraMatrix but no coverslip; one without PuraMatrix but with a coverslip (conventional sandwich culture); and one with neither PuraMatrix nor a coverslip (regular 2D culture). Here, the neuronal ratio (%) is the ratio of the number of neurons to the total cell number (neurons plus astrocytes) in each well. Neuronal ratio was determined by immunostaining neurons with anti-MAP2 and astrocytes with anti-GFAP. Before plating, PuraMatrix was prepared in only two of the four wells in each multiplate. Experiments with cells from different rats were repeated four times. At DIV 38–42 with PuraMatrix, the neuronal ratio was >90% (92±2%, mean ± SE, n = 4) in the coverslip (+) and 86±3% in the coverslip (−) conditions. Our combination method resulted in higher neuronal ratios than without a coverslip in all the 4 replicates. Without PuraMatrix, the neuronal ratio was 97±2% in the coverslip (+) condition, and lowest (64±9%) in the coverslip (−) condition. Regular 2D culture yielded a significantly lower neuronal ratio ($P<0.05$) than all the other conditions, including our combination method.

Two of the 4 replicates were performed as described above: neurons were simultaneously plated into five multiplates, and the neuronal ratio was examined in one plate at each DIV. The neuronal ratios of these replicates were similar and higher than the other two at DIV 38–42, and one replicate is shown in Figure 5. Our combination method with both PuraMatrix and a coverslip resulted in a neuronal ratio of almost 100% for >2 months, with 97% on average and 95% at DIV 69 (Fig. 5A–B). Using PuraMatrix without a coverslip, the neuronal ratio was slightly, but significantly ($P<0.05$) lower at 85% on average and around 80% after DIV 21 (Fig. 5A, C). The specific growth patterns in

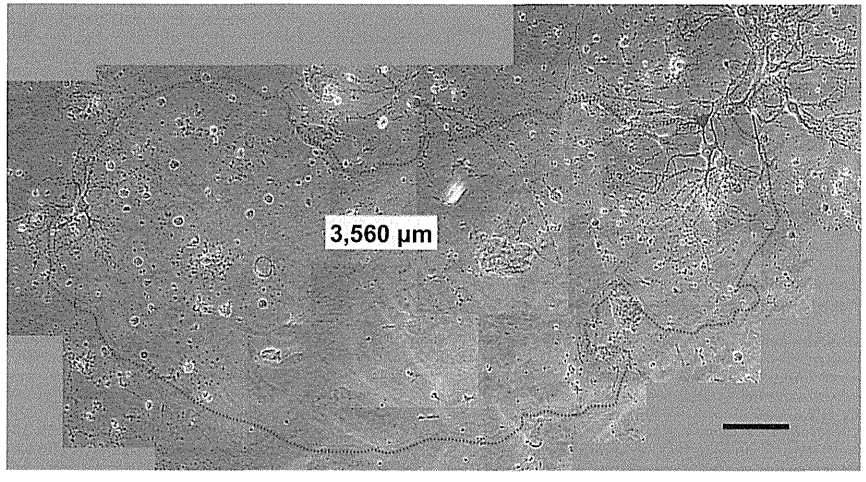

Figure 6. Phase-contrast image of a neuron extending a long neurite (>3,000 μm) at DIV 63. Bar: 100 μm. Neurons from E18 rat hippocampi were plated at 3×10^4 cells/mL in medium #2, and coverslipped 3 h after plating. The neurons show bright, round, and smooth somas, and a characteristic morphology of tapered dendrites with spines and long axons with a uniform diameter (3,560 μm, arrow), suggesting they could survive after the long-term culture for 2 months. Continuity of the axon was confirmed by high-powered microscopy, especially at intersection points of this axon and another neurites (upper) or neurons (left).
doi:10.1371/journal.pone.0102703.g006

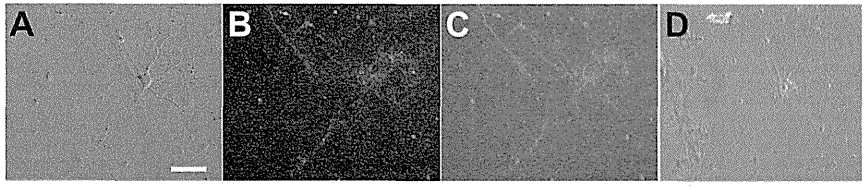

Figure 7. FM1–43 staining of primary neurons at DIV 49. Imaging was performed using the Ti-S (Nikon) (A–C) and BZ-9000 (Keyence) (D) microscopes. Neurons from E18 rat hippocampi were plated at 3×10^4 cells/mL in basic medium #0 on 25% PuraMatrix and coverslipped 3 h after plating. Bar: 50 μm. (A) Phase-contrast image of one neuron. The neuron shows a bright, round, and smooth soma, indicating its viability after long-term culture for 7 weeks. (B) Green fluorescence image of (A), showing synaptic activity. (C) Merged image of the phase-contrast (A) and fluorescence (B) images. (D) Merged image of the phase-contrast and fluorescence images of the same neuron taken using the BZ-9000 microscope. The ultrastructure of the micron-sized spots on the neuron are distinct, indicating synaptic activity.
doi:10.1371/journal.pone.0102703.g007

each condition are shown in Figure 5B–C, E–F, but these are not representative of the average neuronal ratios and viabilities.

Without PuraMatrix, the neuronal ratio varied depending on the presence or absence of a coverslip. With a coverslip, the neuronal ratio was 98% on average. Although this neuronal ratio was slightly, but not significantly higher than our combination method, the neurites were shorter, indicating their depression or regression (Fig. 5D–E). Without a coverslip, the neuronal ratio decreased at first, and then increased again to be 81% on average (Fig. 5D, F). This increase at DIV 42–69 might have occurred because many astrocytes died and detached from the well as the number of DIV increased, while the neurites of the remaining neurons regressed.

In the absence of a coverslip, astrocytes proliferated locally, mainly at the edge of the wells with PuraMatrix (Fig. 5C), and mainly in the center of the wells without PuraMatrix, where both the neurons and astrocytes aggregated (Fig. 5F).

Position within the well

To compare neuronal survival between the center and edge of the well, we calculated the cell viabilities at both positions. Experiments were repeated three times with cells from different rats. With PuraMatrix and a coverslip, viabilities were around 50% in the centers of wells until DIV 35–42; without PuraMatrix but with a coverslip, viabilities were low (20–30%) at DIV 7–69; and without either PuraMatrix or a coverslip, viabilities were several times higher in the center than at the edge because of cell aggregation and glial proliferation. Our combination method with PuraMatrix and a coverslip produced consistent viabilities of around 50% in the centers of wells for 5–6 weeks that were higher than in all other conditions, except for the condition with neither PuraMatrix nor a coverslip. In cultures without PuraMatrix, the difference in cell viabilities between positions was larger, and the viabilities in the center of wells were often significantly higher than at the edge.

Examples of longer neurites

The extremely long neurites obtained with coverslips and PuraMatrix occasionally reached 3,000 μm in basic medium #0 and medium #2. An example neurite of 3,560 μm observed at DIV 63 in medium #2 with a coverslip is shown in Figure 6. This image was selected to show the presence of long neurites, even though the number of living cells in this figure is less than that in the images showing average viability.

Even without a coverslip, neurites of around 3,000 μm were sometimes observed when they migrated into a gap between the two layers of PuraMatrix (e.g. 2,900 μm in #0 at DIV 22). The lower layer of PuraMatrix formed the culture substratum, and another small layer overlapped it.

Synaptic activity

We examined synaptic activity and functional maturation of primary neurons using the endocytotic marker FM1-43 at DIV 49 using two different microscopes, the Ti-S (Nikon) and BZ-9000 (Keyence). Phase-contrast images obtained using the Ti-S microscope (Fig. 7A) indicated neuronal survival, but their ultrastructures, as stained with FM1-43, were unclear (Fig. 7B–C). However, images taken using the BZ-9000 microscope were distinct, and stained puncta on the order of microns could be observed on the neurons (Fig. 7D), demonstrating that active synaptic vesicle recycling was occurring after long-term culture for 7 weeks.

Discussion

Our combination method of the sandwich culture technique using PuraMatrix and coverslips provided the following advantages: (1) long-term culture of primary neurons on a 3D hydrogel without glial feeders for over 2 months at a low density of 3×10^4 cells/mL (8.9×10^3 cells/cm^2); (2) longer neurites (≥3,000 μm) than in culture conditions without a coverslip; (3) an almost pure culture of neurons with an average neuronal ratio of 97%; (4) cell viability ≥40% for 6 weeks and ≥30% for 2 months; and (5) a uniform, single-cell distribution of neurons without aggregation.

Long-term culture on 3D hydrogel without glial feeders at a low density

Our studies suggest the possibility of longer culture periods or lower cell densities without glial feeder layers than previous studies using 2D sandwich culture, including sandwich co-culture with glial cells (<1 month) [4,8,10,1,3,5,6,7,13]. Because our experimental system does not involve a glial feeder, it can be created more simply within a shorter period of several hours, and the evaluation and interpretation of the obtained results is simpler. In addition, our culture system using a 3D nanofibrous hydrogel reproduces *in vivo*-like conditions. 2D culture resulted in undesirable effects (Fig. 5D–F), including neurite depression and low cell viability using a coverslip, and cell aggregation and glial proliferation without a coverslip. These results may be partially due to the use of tissue culture-treated multiplates with no ECM

coating. However, our culture system using a 3D nanofibrous hydrogel provided better results than those obtained in 2D cultures both in this study and in previous studies cited above. Furthermore, our methods may eliminate the need for a coating procedure, as well as the need for glial feeder layers.

Neurite length continued to increase until DIV 42 (Figs. 3B, 4), suggesting that our culture methods were able to suppress regression of axons for 6 weeks. In addition, synaptic activity at DIV 49 was demonstrated (Fig. 7). Namely, our culture methods can maintain axonal growth, neuronal function, and synaptic activity for at least 6–7 weeks.

Longer neurites than in culture conditions without a coverslip

The maximum neurite length was longer with a coverslip than without (Fig. 3), suggesting that the coverslip continued to assist neurite extension during long-term culture >2 months. The longest neurites of primary neurons observed here extended 3,000 μm (Fig. 6). These neurites are 10 times [12] or four times [7] longer than those seen in studies using glial feeders, and 10 *times [18] or four times [28] longer than those seen in studies* using PuraMatrix [18] or polyacrylamide gels [28].

Even without a coverslip, long neurites of around 3,000 μm were sometimes observed to migrate between the two layers of PuraMatrix. In such cases, the upper layer of PuraMatrix may have acted like a coverslip by creating low-oxygen conditions.

The longest neurites stained with MAP2, which were assumed to be dendrites, were approximately 300 μm (Fig. 5B). Therefore, the longest axons were about 10 times longer than the longest dendrites. This result agrees with a previous report [12] and demonstrates that the growth rate of axons was 5–10 times greater than that of dendrites.

Nearly pure neuronal culture without glial proliferation

Our combination method produced a consistently high *neuronal ratio without astrocytes for over 2 months as shown in* Figure 5, significantly higher than without a coverslip. Our results indicated that the effects of the coverslip included the promotion of neuronal growth, suppression of glial proliferation, enhancement of neuronal ratio, and creation of a nearly pure culture for the long term. Since glial proliferation is undesirable in many neuronal cultures, our methods may be greatly beneficial for other neuroscience studies.

The suppression of astrocyte proliferation by PuraMatrix or coverslip placement was indicated by the results of 4 replicates at DIV 38–42 showing that the neuronal ratio for cells with only PuraMatrix and only a coverslip were both significantly higher than that with neither coverslip nor PuraMatrix. Glial proliferation with neither PuraMatrix nor a coverslip is in agreement with previous studies, which showed that neurons grew well on collagen [23] or polyacrylamide [28] gels, whereas glia proliferated on 2D coated surfaces.

A sandwich culture method using coverslips and cytosine arabinoside has been proposed [10]. The neuronal ratio achieved with this method was 95% at DIV 5 at a density of 10^5 cells/mL. However, those cultures showed short-term survival at high density, and cytosine arabinoside has toxic effects. In this regard, our sandwich culture method is favorable because it can reproduce *in vivo*-like low-oxygen conditions without a toxic substance.

Cell viability greater than 30% for 2 months

Cell viability of ≥30% for 2 months or ≥40% for 6 weeks was not significantly different from that without a coverslip, as shown in Fig. 3, suggesting that our sandwich culture method did not decrease neuronal survival. The viability decreased to approximately 50% within several days, but was still higher than that reported in previous studies with cells at the same low densities as ours [4,5,6,7,9,10]. After that time, our methods provided an extremely slow decrease in viability for >2 months, which differs from previous studies.

Although the viability of cells in our study was relatively low (< 50%), it remained higher than that reported in previous studies. Because neurons cultured using our method exhibited normal development (Fig. 2), long-term axonal elongation (≥3,000 μm), synaptic activity at DIV 49, and survival of many neurons without astrocytes, this technique represents an advance over existing culture methods and provides a system for creating *in vivo*-like culture conditions.

The cell viability shown in Figure 3A was as great or greater than that in the 4 replicates that underwent repeated microscopy and in the "Comparison of culture media" section, possibly because microscopy was performed only once in the experiment shown in Figure 3, but several times in the other experiments. Microscopy has an adverse effect on cultured neurons owing to the optical illumination and change in temperature and CO_2 concentration. Based on the 12 replicates, microscopy before DIV 14 appeared to be especially harmful.

Likewise, the maximum neurite lengths shown in Figure 3B were longer than those in the "Comparison of culture media" section, and neuronal ratios shown in Figure 5 were highest in the 4 replicates, probably because of the same reasons. Thus, we believe the results shown in Figs. 3–5 are the most accurate.

Uniform, single-cell distribution of neurons

The combination approach also provided a uniform distribution of primary neurons and high viabilities in the center of the well (around 50% for 5–6 weeks). Furthermore, a near single-cell distribution was achieved, and unfavorable aggregation was suppressed over the long term (>2 months, Fig. 2). This culture condition of a uniform, single-cell distribution will be greatly advantageous for long-term research of individual neurons and neuronal networks.

In a previous study [4], most neurons sandwiched by a coverslip survived along its edge, probably because the oxygen in the center was too low. In contrast, our combination method provided a uniform distribution across the well, possibly because of the ultrastructure of PuraMatrix. That is, the fibrous nanostructure and rough surface, with a maximum height difference of <40 μm (Fig. 1), may have improved the microenvironment and the microgradients of oxygen, paracrine factors, and other chemical substances.

Synaptic activity

After long-term culture for 7 weeks using our culture methods, *synaptic vesicle turnover was detected by FM1-43 staining*, as shown in Figure 7. Stained spots of 1–2 μm indicate the presence of active presynaptic terminals, suggesting that our methods were able to generate and maintain active, functional synapses over the long term. Extremely small spots were visualized using the BZ-9000 microscope as discussed below.

Other culture conditions

Basic medium #0 provided much longer neurites (>1,600 μm) than DMEM/F12 (around 500 μm) and 2% FBS/N2/MEM (< 100 μm) (Table 1). The comparable supporting effects of media #0, #1, #2, and #2/1 on neuronal outgrowth seem to be due to the common components, Neurobasal medium and B27, rather

than L-glutamine, glutamic acid, or GlutaMAX. Based on the results for conditions with neither a coverslip nor PuraMatrix, basic medium #0 had the same beneficial effects as coverslips and PuraMatrix. Combining all components of our method (coverslips, PuraMatrix, and culture medium) should be used for best results.

Our finding that 25% PuraMatrix resulted in significantly longer neurites (1.7–1.8-fold) in PC12 and primary neurons than 50% or 100% suggests that it promotes neuronal differentiation, which is consistent with the results of previous studies [20,28].

In addition, we found that the earlier a coverslip was placed, the faster neurons extended neurites and the faster they regressed, with no effect on cell viability. Few previous studies have compared different coverslip placement or inverting time points, but 1 h [4,8], 1.5 h [10], 3–4 h (the same as our study) [1,3], and 24 h [29] after plating have been reported.

Regarding the embryonic day of isolation of hippocampal neurons, E18 rat hippocampal neurons developed neurites of more than twice the length of those developed by E19 neurons in #0, in agreement with the general principle that the younger an organism is, the higher its regenerative capacity.

Microscopy was sometimes repeated, and the same neurites may therefore have been measured on different days. However, this likely did not affect the comparisons of culture conditions. If culture conditions were suboptimal, neurites that initially extended would regress and become shorter at earlier times. The extension of neurites over the long-term indicated that the culture conditions were appropriate. In the experiments shown in Figures 3–5, where microscopy was only performed once, the benefits of the coverslip+ over the coverslip– condition were even greater than in the other experiments with repeated microscopy. In addition, we performed unpaired t-tests to assess the significance of differences in neurite length and cell viability between different groups, such as coverslip+ and coverslip–; these two groups were independent and did not include the same neurites that may be measured repeatedly.

3D culture imaging

Image quality in our culture system is decreased by the rough, thick, and semi-opaque 3D substrates. In addition, it is difficult to focus on cells or neurites extending three-dimensionally on the rough surface of 3D substrates. Furthermore, dyes tend to be adsorbed by 3D substrates non-specifically, raising the fluorescent background. If 3D substrates are washed too many times to reduce background noise, they can lose mechanical integrity and soft substrates, as used here, may collapse.

In our studies, the phase-contrast and fluorescence images (Figs. 2, 3C, 5, 6, 7A–C) might be unfocused or have high-background compared with those in 2D culture. We used the LIVE/DEAD Viability/Cytotoxicity Kit (Figs. 2D, 2G, 3D, 4) because neurons could be stained clearly after a single-step assay, and even neurites extending three-dimensionally on PuraMatrix could be traced (Fig. 4A).

We used a BZ-9000 microscope after staining with FM1–43. Although synaptic vesicles are 1–2 μm in size and difficult to identify using a normal microscope (Fig. 7A–C), we were able to take high-resolution images using the BZ-9000 microscope without any preprocessing or complicated operations (Fig. 7D).

We also used a digital microscope to analyze the surface roughness of PuraMatrix in our culture conditions. Although SEM or TEM is often used for 3D analysis, preprocessing is required, and the images may contain artifacts from those steps different from those in culture conditions. With other non-destructive optical 3D microscopes, measuring transparent surfaces like PuraMatrix with neurons in medium is difficult. However, by using a digital microscope (VHX2000/1100, Keyence), we were able to determine the surface roughness of PuraMatrix as shown in Figure 1. These microscopes and fluorescence dyes have good potential for use in 3D culture imaging and analysis.

Applicability and limitations

Because our culture system was capable of producing cells with long axons (≥3,000 μm), it may prove useful as an *in vitro* culture system for studying axonal regeneration of CNS neurons *in vivo*. As shown in Figure 5, glial proliferation was also suppressed, suggesting the possibility of suppressing glial scar formation, which is thought to be one of the factors that inhibit the regeneration of CNS neurons. Namely, our culture system has the potential to be a significant advance in regenerative medicine and tissue engineering because CNS neuronal regeneration *in vivo* following nerve injury (traumatic brain injury or spinal cord injury) is extremely poor and motor functional recovery is limited.

Several limitations of the present study should be discussed. Only hippocampal neurons and PC12 cells from rats were used in this study. To strengthen the benefits and applicability of our method, it should be applied to various other types of cells, such as motor neurons, and for 3D differentiation culture of induced pluripotent stem cells or embryonic stem cells. Regarding the maximum neurite length, we did not measure all neurites, but subjectively selected long neurites. However, long neurites were typically observed in limited areas of the well where neurons were sparse. Fluorescence images also helped us detect long neurites. It would be very difficult to measure the lengths of all neurites because they overlap and exist in 3D. However, comparisons of neurite lengths measured by the same methods would not likely affect the results showing the benefits of our culture methods over other conditions.

Conclusions

Our combination approach, using 25% PuraMatrix and coverslips, with the medium and timing parameters described above, provided the best results for the long term, nearly pure culture of rat hippocampal neurons. These techniques promoted neuronal survival and neurite extension, suppressed glial proliferation and cell aggregation, and reproduced *in vivo*-like culture conditions.

Author Contributions

Conceived and designed the experiments: AK YS. Performed the experiments: AK. Analyzed the data: AK. Contributed reagents/materials/analysis tools: AK YS. Wrote the paper: AK.

References

1. Kaech S, Banker G (2006) Culturing hippocampal neurons. Nat Protoc 1: 2406–2415.
2. Banker G, Goslin K (1998) Culturing nerve cells, second ed. Cambridge, MA: MIT press.
3. Goslin K, Asmussen H, Banker G (1998) Rat hippocampal neurons in low-density culture. In: Banker G, Goslin K, editors. Culturing nerve cells. Cambridge, MA: MIT press. pp. 339–370.
4. Brewer GJ, Cotman CW (1989) Survival and growth of hippocampal neurons in defined medium at low density: advantages of a sandwich culture technique or low oxygen. Brain Res 494: 65–74.
5. Banker GA (1980) Trophic interactions between astroglial cells and hippocampal neurons in culture. Science 209: 809–810.
6. Banker GA, Cowan WM (1977) Rat hippocampal neurons in dispersed cell culture. Brain Res 126: 397–425.
7. Banker GA, Cowan WM (1979) Further observations on hippocampal neurons in dispersed cell culture. J Comp Neur 187: 469–494.
8. Brewer GJ, Torricelli JR, Evege EK, Price PJ (1993) Optimized survival of hippocampal neurons in B27-supplemented Neurobasal, a new serum-free medium combination. J Neurosci Res 35: 567–576.
9. Brewer GJ, Torricelli J, Evege EK, Price PJ (1994) Neurobasal medium/B27 supplement: A new serum-free medium combination for survival of neurons. Focus 16: 6–9.
10. Lucius R, Mentlein R (1995) Development of a culture system for pure rat neurons: advantages of a sandwich technique. Ann Anat 177: 447–454.
11. Khan MZ, Shimizu S, Patel JP, Nelson A, Le MT, et al. (2005) Regulation of neuronal P53 activity by CXCR4. Mol Cell Neurosci 30: 58–66.
12. Dotti CG, Sullivan CA, Banker GA (1988) The establishment of polarity by hippocampal neurons in culture. J Neurosci 8: 1454–1468.
13. Chen Y, Stevens B, Chang J, Millbrandt J, Barres BA, et al. (2008) NS21: Re-defined and modified supplement B27 for neuronal cultures. J Neurosci Meth 171: 239–247.
14. Cook A, Hippensteel R, Shimizu S, Nicolai J, Fatatis A, et al. (2010) Interactions between chemokines: regulation of fractalkine/CX_3CL1 homeostasis by SDF/CXCL12 in cortical neurons. J Biol Chem 285: 10563–10571.
15. Meucci O, Fatatis A, Simen AA, Bushell TJ, Gray PW, et al. (1998) Chemokines regulate hippocampal neuronal signaling and gp120 neurotoxicity. Proc Natl Acad Sci USA 95: 14500–14505.
16. Meucci O, Miller RJ (1996) gp120-induced neurotoxicity in hippocampal pyramidal neuron cultures: protective action of TGF-β1. J Neurosci 16: 4080–4088.
17. LaPlaca MC, Vernekar VN, Shoemaker JT, Cullen DK (2010) Three-dimensional neuronal cultures. In: Berthiaume F, Morgan J, editors. Methods in bioengineering: 3D tissue engineering. Norwood, MA: Artech House. pp. 187–204.
18. Holmes TC, de Lacalle S, Su X, Liu G, Rich A, et al. (2000) Extensive neurite outgrowth and active synapse formation on self-assembling peptide scaffolds. Proc Natl Acad Sci USA 97: 6728–6733.
19. Semino CE, Kasahara J, Hayashi Y, Zhang S (2004) Entrapment of migrating hippocampal neural cells in three-dimensional peptide nanofiber scaffold. Tissue Eng 10: 643–655.
20. Thonhoff JR, Lou DI, Jordan PM, Zhao X, Wu P (2008). Compatibility of human fetal neural stem cells with hydrogel biomaterials *in vitro*. Brain Res 1187: 42–51.
21. Gulati SC, Sood SC, Bali IM, Kak VK (1980) Cerebral metabolism following brain injury. I. Acid-base and pO_2 changes. Acta Neurochir 53: 39–46.
22. Zupping R (1972) Cerebral metabolism in patients with intracranial tumors. J Neurosurg 36: 451–462.
23. Harris WA, Holt CE, Smith TA, Gallenson N (1985) Growth cones of developing retinal cells *in vivo*, on culture surfaces, and in collagen matrices. J Neurosci Res 13: 101–122.
24. Grill RJ Jr, Pixley SK (1993) 2-Mercaptoethanol is a survival factor for olfactory, cortical and hippocampal neurons in short-term dissociated cell culture. Brain Res 613: 168–172.
25. Ishii K, Katayama M, Hori K, Yodoi J, Nakanishi T (1993) Effects of 2-mercaptoethanol on survival and differentiation of fetal mouse brain neurons cultured *in vitro*. Neurosci Lett 163: 159–162.
26. Sango K, Oohira A, Ajiki K, Tokashiki A, Horie M, et al. (2003) Phosphacan and neurocan are repulsive substrata for adhesion and neurite extension of adult rat dorsal root ganglion neurons *in vitro*. Exp Neurol 182: 1–11.
27. Hansen MB, Jespersen SN, Leigland LA, Kroenke CD (2013) Using diffusion anisotropy to characterize neuronal morphology in gray matter: the orientation distribution of axons and dendrites in the NeuroMorpho.org database. Front Integr Neurosci 7: 31 doi:10.3389/fnint.2013.00031.
28. Flanagan LA, Ju Y-E, Marg B, Osterfield M, Jamney PA (2002) Neurite branching on deformable substrates. Neuroreport 13: 2411–2415.
29. Scherer J, Friedrich G, Schnitzer J (1995) Differentiation and maturation of rabbit retinal oligodendrocyte precursor cells *in vitro*. Dev Brain Res 89: 214–226.